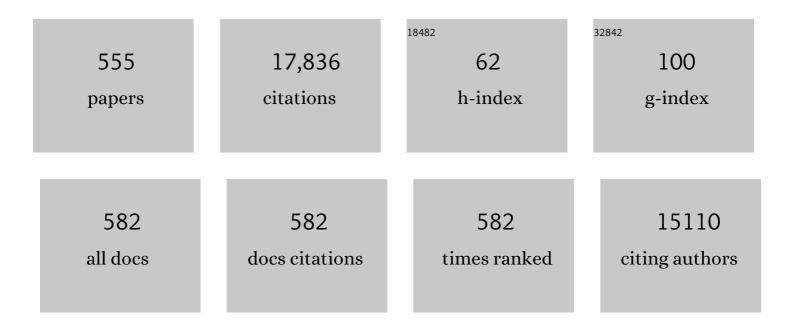
List of Publications by Year in descending order

Source: https://exaly.com/author-pdf/8702041/publications.pdf Version: 2024-02-01



#	Article	IF	CITATIONS
1	Polymers of intrinsic microporosity (PIMs) in sensing and in electroanalysis. Current Opinion in Chemical Engineering, 2022, 35, 100765.	7.8	10
2	Polymer indicator displacement assay: electrochemical glucose monitoring based on boronic acid receptors and graphene foam competitively binding with poly-nordihydroguaiaretic acid. Analyst, The, 2022, 147, 661-670.	3.5	3
3	Nanostructuring Electrode Surfaces and Hydrogels for Enhanced Thermocapacitance. ACS Applied Nano Materials, 2022, 5, 438-445.	5.0	4
4	Crosslinked xylose-based polyester as a bio-derived and degradable solid polymer electrolyte for Li ⁺ -ion conduction. Journal of Materials Chemistry A, 2022, 10, 6796-6808.	10.3	11
5	TiO ₂ nanocrystal rods on titanium microwires: growth, vacuum annealing, and photoelectrochemical oxygen evolution. New Journal of Chemistry, 2022, 46, 8385-8392.	2.8	2
6	Foam Synthesis of Nickel/Nickel (II) Hydroxide Nanoflakes Using Double Templates of Surfactant Liquid Crystal and Hydrogen Bubbles: A High-Performance Catalyst for Methanol Electrooxidation in Alkaline Solution. Nanomaterials, 2022, 12, 879.	4.1	5
7	Electrochemical sensors based on metal nanoparticles with biocatalytic activity. Mikrochimica Acta, 2022, 189, 172.	5.0	35
8	Effects of g-C ₃ N ₄ Heterogenization into Intrinsically Microporous Polymers on the Photocatalytic Generation of Hydrogen Peroxide. ACS Applied Materials & Interfaces, 2022, 14, 19938-19948.	8.0	17
9	Current Insight into 3D Printing in Solidâ€State Lithiumâ€Ion Batteries: A Perspective. Batteries and Supercaps, 2022, 5, .	4.7	19
10	lonic diode desalination: Combining cationic Nafionâ"¢ and anionic Sustainionâ"¢ rectifiers. Micro and Nano Engineering, 2022, 16, 100157.	2.9	6
11	The influence of metallic Bi in BiVO4 semiconductor for artificial photosynthesis. Journal of Alloys and Compounds, 2021, 851, 156912.	5.5	19
12	Atomic scale surface modification of TiO ₂ 3D nano-arrays: plasma enhanced atomic layer deposition of NiO for photocatalysis. Materials Advances, 2021, 2, 273-279.	5.4	4
13	Photo-Chlorine Production with Hydrothermally Grown and Vacuum-Annealed Nanocrystalline Rutile. Electrocatalysis, 2021, 12, 65-77.	3.0	5
14	Hematite photoelectrodes grown on porous CuO–Sb2O5–SnO2 ceramics for photoelectrochemical water splitting. Solar Energy Materials and Solar Cells, 2021, 221, 110886.	6.2	7
15	Semiconductor photoelectroanalysis and photobioelectroanalysis: A perspective. TrAC - Trends in Analytical Chemistry, 2021, 135, 116154.	11.4	9
16	Indirect Formic Acid Fuel Cell Based on a Palladium or Palladiumâ€Alloy Film Separating the Fuel Reaction and Electricity Generation. ChemElectroChem, 2021, 8, 378-385.	3.4	8
17	Utilization of a Pt(<scp>ii</scp>) di-yne chromophore incorporating a 2,2′-bipyridine-5,5′-diyl spacer as a chelate to synthesize a green and red emitting d–f–d heterotrinuclear complex. Dalton Transactions, 2021, 50, 1465-1477.	3.3	16
18	Electrochemically Induced Mesomorphism Switching in a Chlorpromazine Hydrochloride Lyotropic Liquid Crystal. ACS Omega, 2021, 6, 4630-4640.	3.5	1

#	Article	IF	CITATIONS
19	Microscale Ionic Diodes: An Overview. Electroanalysis, 2021, 33, 1398-1418.	2.9	15
20	Recent Advances in Paired Electrosynthesis. Chemical Record, 2021, 21, 2585-2600.	5.8	46
21	Electrodeposition of tin onto a silver textile electrode for Barbier-type electro-organic synthesis of homoallylic alcohols. Surfaces and Interfaces, 2021, 24, 101085.	3.0	0
22	Ionic Diode and Molecular Pump Phenomena Associated with Caffeic Acid Accumulated into an Intrinsically Microporous Polyamine (PIMâ€EAâ€TB). ChemElectroChem, 2021, 8, 2044-2051.	3.4	7
23	Sizeâ€Selective Photoelectrochemical Reactions in Microporous Environments: Clark Probe Investigation of Pt@gâ€C ₃ N ₄ Embedded into Intrinsically Microporous Polymer (PIMâ€1). ChemElectroChem, 2021, 8, 3499-3505.	3.4	6
24	Non-enzymatic electrochemical cholesterol sensor based on strong host-guest interactions with a polymer of intrinsic microporosity (PIM) with DFT study. Analytical and Bioanalytical Chemistry, 2021, 413, 6523-6533.	3.7	7
25	Thermogalvanic and Thermocapacitive Behavior of Superabsorbent Hydrogels for Combined Low-Temperature Thermal Energy Conversion and Harvesting. ACS Applied Energy Materials, 2021, 4, 11204-11214.	5.1	21
26	Effective electroosmotic transport of water in an intrinsically microporous polyamine (PIM-EA-TB). Electrochemistry Communications, 2021, 130, 107110.	4.7	5
27	Novel hierarchical structure of MoS2/TiO2/Ti3C2Tx composites for dramatically enhanced electromagnetic absorbing properties. Journal of Advanced Ceramics, 2021, 10, 1042-1051.	17.4	96
28	Solvent-controlled O ₂ diffusion enables air-tolerant solar hydrogen generation. Energy and Environmental Science, 2021, 14, 5523-5529.	30.8	6
29	Catechin or quercetin guests in an intrinsically microporous polyamine (PIM-EA-TB) host: accumulation, reactivity, and release. RSC Advances, 2021, 11, 27432-27442.	3.6	4
30	Polymers of Intrinsic Microporosity in the Design of Electrochemical Multicomponent and Multiphase Interfaces. Analytical Chemistry, 2021, 93, 1213-1220.	6.5	19
31	Hydrogen Peroxide Versus Hydrogen Generation at Bipolar Pd/Au Nano-catalysts Grown into an Intrinsically Microporous Polyamine (PIM-EA-TB). Electrocatalysis, 2021, 12, 771-784.	3.0	3
32	Graphene oxide and starch gel as a hybrid binder for environmentally friendly high-performance supercapacitors. Communications Chemistry, 2021, 4, .	4.5	16
33	Effects of dissolved gases on partial anodic passivation phenomena at copper microelectrodes immersed in aqueous NaCl. Journal of Electroanalytical Chemistry, 2020, 872, 113589.	3.8	3
34	Bacteriophage M13 Aggregation on a Microhole Poly(ethylene terephthalate) Substrate Produces an Anionic Current Rectifier: Sensitivity toward Anionic versus Cationic Guests. ACS Applied Bio Materials, 2020, 3, 512-521.	4.6	11
35	Switching Anionic and Cationic Semipermeability in Partially Hydrolyzed Polyacrylonitrile: A pH-Tunable Ionic Rectifier. ACS Applied Materials & Interfaces, 2020, 12, 3214-3224.	8.0	13
36	Voltammetric monitoring of a solid-liquid phase transition in N,N,N′,N′-tetraoctyl-2,6-diamino-9,10-anthraquinone (TODAQ). Journal of Solid State Electrochemistry, 2020, 24, 11-16.	2.5	0

#	Article	IF	CITATIONS
37	Linking the Cu(II/I) and the Ni(IV/II) Potentials to Subsequent Passive Film Breakdown for a Cuâ^'Ni Alloy in Aqueous 0.5â€M NaCl. ChemElectroChem, 2020, 7, 195-200.	3.4	2
38	A BiVO4 photoanode grown on porous and conductive SnO2 ceramics for water splitting driven by solar energy. Ceramics International, 2020, 46, 9040-9049.	4.8	14
39	CRP-binding bacteriophage as a new element of layer-by-layer assembly carbon nanofiber modified electrodes. Bioelectrochemistry, 2020, 136, 107629.	4.6	10
40	Surface modified carbon nanomats provide cationic and anionic rectifier membranes in aqueous electrolyte media. Electrochimica Acta, 2020, 354, 136750.	5.2	5
41	Polymer of intrinsic microporosity (PIM) films and membranes in electrochemical energy storage and conversion: A mini-review. Electrochemistry Communications, 2020, 118, 106798.	4.7	45
42	Direct and indirect light energy harvesting with films of ambiently deposited ZnO nanoparticles. Applied Surface Science, 2020, 527, 146927.	6.1	3
43	Unmasking the Latent Passivating Roles of Ni(OH) ₂ on the Performance of Pd–Ni Electrocatalysts for Alkaline Ethanol Fuel Cells. ACS Applied Energy Materials, 2020, 3, 8786-8802.	5.1	31
44	Rectification effects of Nafion-backed micropore-voltammograms by difference in migrational modes. Electrochimica Acta, 2020, 358, 136839.	5.2	9
45	Role of dissolved oxygen in nitroarene reduction by a heterogeneous silver textile catalyst in water. New Journal of Chemistry, 2020, 44, 17780-17790.	2.8	7
46	Photoelectroanalytical Oxygen Detection with Titanate Nanosheet – Platinum Hybrids Immobilised into a Polymer of Intrinsic Microporosity (PIMâ€1). Electroanalysis, 2020, 32, 2756-2763.	2.9	5
47	Covalently Linked Polyoxometalate–Polypyrrole Hybrids: Electropolymer Materials with Dual-Mode Enhanced Capacitive Energy Storage. Macromolecules, 2020, 53, 11120-11129.	4.8	12
48	Future challenges in electrochemistry: linking membrane-based solar energy conversion mechanisms to water harvesting. Journal of Solid State Electrochemistry, 2020, 24, 2137-2140.	2,5	0
49	Indirect photo-electrochemical detection of carbohydrates with Pt@g-C3N4 immobilised into a polymer of intrinsic microporosity (PIM-1) and attached to a palladium hydrogen capture membrane. Bioelectrochemistry, 2020, 134, 107499.	4.6	12
50	Review—The Development of Wearable Polymer-Based Sensors: Perspectives. Journal of the Electrochemical Society, 2020, 167, 037566.	2.9	76
51	An AC-driven desalination/salination system based on a Nafion cationic rectifier. Desalination, 2020, 480, 114351.	8.2	16
52	Voltammetric detection of vitamin B1 (thiamine) in neutral solution at a glassy carbon electrode <i>via in situ</i> pH modulation. Analyst, The, 2020, 145, 1903-1909.	3.5	10
53	The immobilisation and reactivity of Fe(CN)63â^'/4â^' in an intrinsically microporous polyamine (PIM-EA-TB). Journal of Solid State Electrochemistry, 2020, 24, 2797-2806.	2.5	14
54	Indirect (hydrogen-driven) electrodeposition of porous silver onto a palladium membrane. Journal of Solid State Electrochemistry, 2020, 24, 2789-2796.	2.5	1

#	Article	IF	CITATIONS
55	Charge Transfer Hybrids of Graphene Oxide and the Intrinsically Microporous Polymer PIM-1. ACS Applied Materials & Interfaces, 2019, 11, 31191-31199.	8.0	9
56	A hematite photoelectrode grown on porous and conductive SnO2 ceramics for solar-driven water splitting. International Journal of Hydrogen Energy, 2019, 44, 19667-19675.	7.1	16
57	Ferrocene-Containing Polycarbosilazanes via the Alkaline-Earth-Catalyzed Dehydrocoupling of Silanes and Amines. Organometallics, 2019, 38, 3629-3648.	2.3	26
58	Carbon-based quantum particles: an electroanalytical and biomedical perspective. Chemical Society Reviews, 2019, 48, 4281-4316.	38.1	187
59	Polymers of Intrinsic Microporosity in Triphasic Electrochemistry: Perspectives. ChemElectroChem, 2019, 6, 4332-4342.	3.4	25
60	Carbon Nanofibers Provide a Cationic Rectifier Material: Specific Electrolyte Effects, Bipolar Reactivity, and Prospect for Desalination. ChemElectroChem, 2019, 6, 3145-3153.	3.4	8
61	Voltammetric characterisation of diferrocenylborinic acid in organic solution and in aqueous media when immobilised into a titanate nanosheet film. Dalton Transactions, 2019, 48, 11200-11207.	3.3	2
62	Utilization of Ternary Europium Complex for Organic Electroluminescent Devices and as a Sensitizer to Improve Electroluminescence of Red-Emitting Iridium Complex. Inorganic Chemistry, 2019, 58, 8316-8331.	4.0	38
63	Extraction of hydrophobic analytes from organic solution into a titanate 2D-nanosheet host: Electroanalytical perspectives. Analytica Chimica Acta: X, 2019, 1, 100001.	1.0	3
64	Processes associated with ionic current rectification at a 2D-titanate nanosheet deposit on a microhole poly(ethylene terephthalate) substrate. Journal of Solid State Electrochemistry, 2019, 23, 1237-1248.	2.5	12
65	Success and failure in the incorporation of gold nanoparticles inside ferri/ferrocyanide thermogalvanic cells. Electrochemistry Communications, 2019, 102, 41-45.	4.7	29
66	Photoelectrochemistry of immobilised Pt@g-C3N4 mediated by hydrogen and enhanced by a polymer of intrinsic microporosity PIM-1. Electrochemistry Communications, 2019, 103, 1-6.	4.7	18
67	Electrodes modified with bacteriophages and carbon nanofibres for cysteine detection. Sensors and Actuators B: Chemical, 2019, 287, 78-85.	7.8	24
68	Multiphase Methods in Organic Electrosynthesis. Accounts of Chemical Research, 2019, 52, 3325-3338.	15.6	25
69	Biphasic Voltammetry and Spectroelectrochemistry in Polymer of Intrinsic Microporosity—4-(3-Phenylpropyl)-Pyridine Organogel/Aqueous Electrolyte Systems: Reactivity of MnPc Versus MnTPP. Electrocatalysis, 2019, 10, 295-304.	3.0	4
70	Pyro-electrolytic water splitting for hydrogen generation. Nano Energy, 2019, 58, 183-191.	16.0	50
71	Cationic Rectifier Based on a Graphene Oxide-Covered Microhole: Theory and Experiment. Langmuir, 2019, 35, 2055-2065.	3.5	25
72	Polymer of Intrinsic Microporosity (PIMâ€7) Coating Affects Triphasic Palladium Electrocatalysis. ChemElectroChem, 2019, 6, 4307-4317.	3.4	9

#	Article	IF	CITATIONS
73	Triphasic Nature of Polymers of Intrinsic Microporosity Induces Storage and Catalysis Effects in Hydrogen and Oxygen Reactivity at Electrode Surfaces. ChemElectroChem, 2019, 6, 252-259.	3.4	30
74	Non-invasive, transdermal, path-selective and specific glucose monitoring via a graphene-based platform. Nature Nanotechnology, 2018, 13, 504-511.	31.5	242
75	Electrochemically Driven Câ^'H Hydrogen Abstraction Processes with the Tetrachloroâ€Phthalimidoâ€Nâ€Oxyl (Cl ₄ PINO) Catalyst. Electroanalysis, 2018, 30, 1706-1713.	2.9	6
76	Galvanic exchange platinization reveals laser-inscribed pattern in 3D-LAM-printed steel. Journal of Solid State Electrochemistry, 2018, 22, 1755-1762.	2.5	1
77	Cationic diodes by hot-pressing of Fumasep FKS-30 ionomer film onto a microhole in polyethylene terephthalate (PET). Journal of Electroanalytical Chemistry, 2018, 815, 114-122.	3.8	10
78	lonic Transport in Microhole Fluidic Diodes Based on Asymmetric Ionomer Film Deposits. ChemElectroChem, 2018, 5, 897-901.	3.4	30
79	pH effects on molecular hydrogen storage in porous organic cages deposited onto platinum electrodes. Journal of Electroanalytical Chemistry, 2018, 819, 46-50.	3.8	5
80	Nano- and micro-gap electrochemical transducers: Novel benchtop fabrication techniques and electrical migration effects. Current Opinion in Electrochemistry, 2018, 7, 15-21.	4.8	4
81	Generator–collector electrochemical sensor configurations based on track-Etch membrane separated platinum leaves. Sensors and Actuators B: Chemical, 2018, 255, 2904-2909.	7.8	1
82	Residual Energy Harvesting from Light Transients Using Hematite as an Intrinsic Photocapacitor in a Symmetrical Cell. ACS Applied Energy Materials, 2018, 1, 38-42.	5.1	5
83	Linking the Cu(II/I) potential to the onset of dynamic phenomena at corroding copper microelectrodes immersed in aqueous 0.5â€ ⁻ M NaCl. Electrochimica Acta, 2018, 260, 348-357.	5.2	9
84	One-step preparation of microporous Pd@cPIM composite catalyst film for triphasic electrocatalysis. Electrochemistry Communications, 2018, 86, 17-20.	4.7	14
85	Electroanalysis in 2Dâ€TiO ₂ Nanosheet Hosts: Electrolyte and Selectivity Effects in Ferroceneboronic Acid – Saccharide Binding. Electroanalysis, 2018, 30, 1303-1310.	2.9	10
86	In Situ Ultrasonic Dispersion in Multiphase Electrolysis Systems. Electrochemical Society Interface, 2018, 27, 59-62.	0.4	1
87	The thermoelectrochemistry of the aqueous iron(<scp>ii</scp>)/iron(<scp>iii</scp>) redox couple: significance of the anion and pH in thermogalvanic thermal-to-electrical energy conversion. Sustainable Energy and Fuels, 2018, 2, 2717-2726.	4.9	75
88	Dicopper(I) Complexes Incorporating Acetylide-Functionalized Pyridinyl-Based Ligands: Synthesis, Structural, and Photovoltaic Studies. Inorganic Chemistry, 2018, 57, 12113-12124.	4.0	18
89	Electrochemical and Kinetic Insights into Molecular Water Oxidation Catalysts Derived from Cp*lr(pyridineâ€alkoxide) Complexes. ChemCatChem, 2018, 10, 4280-4291.	3.7	16
90	Contrasting transient photocurrent characteristics for thin films of vacuum-doped "grey―TiO2 and "grey―Nb2O5. Applied Catalysis B: Environmental, 2018, 237, 339-352.	20.2	21

#	Article	IF	CITATIONS
91	Voltammetric characteristics of hydrous Fe(III) oxide embedded into Nafion and immobilised onto a screen-printed carbon electrode: binding of arsenate versus phosphate. Journal of Solid State Electrochemistry, 2018, 22, 3059-3067.	2.5	2
92	Continuous low temperature synthesis of MAPbX ₃ perovskite nanocrystals in a flow reactor. Reaction Chemistry and Engineering, 2018, 3, 640-644.	3.7	41
93	Platinum Nanoparticle Inclusion into a Carbonized Polymer of Intrinsic Microporosity: Electrochemical Characteristics of a Catalyst for Electroless Hydrogen Peroxide Production. Nanomaterials, 2018, 8, 542.	4.1	8
94	A happy couple. Nature Catalysis, 2018, 1, 484-485.	34.4	1
95	Enhancing activity in a nanostructured BiVO4 photoanode with a coating of microporous Al2O3. Applied Catalysis B: Environmental, 2017, 200, 133-140.	20.2	26
96	Electrothermal Annealing of Catalytic Platinum Microwire Electrodes: Towards Membraneâ€Free pHâ€7 Glucose Microâ€Fuel Cells. Electroanalysis, 2017, 29, 38-44.	2.9	6
97	Dual-Plate Gold-Gold Microtrench Electrodes for Generator-Collector Voltammetry without Supporting Electrolyte. Electrochimica Acta, 2017, 224, 487-495.	5.2	5
98	Ionic Diodes Based on Regenerated αâ€Cellulose Films Deposited Asymmetrically onto a Microhole. ChemistrySelect, 2017, 2, 871-875.	1.5	7
99	Reaction-based indicator displacement assay (RIA) for the colorimetric and fluorometric detection of hydrogen peroxide. Organic Chemistry Frontiers, 2017, 4, 1058-1062.	4.5	25
100	Free‣tanding Phytantriol Q ²²⁴ Cubicâ€Phase Films: Resistivity Monitoring and Switching. ChemElectroChem, 2017, 4, 1172-1180.	3.4	11
101	Vacuum-annealing induces sub-surface redox-states in surfactant-structured α-Fe2O3 photoanodes prepared by ink-jet printing. Applied Catalysis B: Environmental, 2017, 211, 289-295.	20.2	14
102	Confining Nanopore Bipolar Electrochemical Processes to Give Pattern in Space and Time. ChemElectroChem, 2017, 4, 2137-2139.	3.4	2
103	Redox reactivity at silver microparticle—glassy carbon contacts under a coating of polymer of intrinsic microporosity (PIM). Journal of Solid State Electrochemistry, 2017, 21, 2141-2146.	2.5	13
104	Microwave-Electrochemical Deposition of a Fe-Co Alloy with Catalytic Ability in Hydrogen Evolution. Electrochimica Acta, 2017, 235, 480-487.	5.2	19
105	A Cationic Diode Based on Asymmetric Nafion Film Deposits. ACS Applied Materials & Interfaces, 2017, 9, 11272-11278.	8.0	42
106	Cellulose ionics: switching ionic diode responses by surface charge in reconstituted cellulose films. Analyst, The, 2017, 142, 3707-3714.	3.5	15
107	Ionic Diode Characteristics at a Polymer of Intrinsic Microporosity (PIM) Nafion "Heterojunction― Deposit on a Microhole Poly(ethyleneâ€ŧerephthalate) Substrate. Electroanalysis, 2017, 29, 2217-2223.	2.9	11
108	Voltammetric Chloride Sensing Based on Trace-Level Mercury Impregnation Into Amine-Functionalized Carbon Nanoparticle Films. IEEE Sensors Journal, 2017, 17, 5437-5443.	4.7	5

#	Article	IF	CITATIONS
109	Highly conductive nano-silver textile for sensing hydrogen peroxide. Journal of Electroanalytical Chemistry, 2017, 799, 473-480.	3.8	16
110	Carbonization of polymers of intrinsic microporosity to microporous heterocarbon: Capacitive pH measurements. Applied Materials Today, 2017, 9, 136-144.	4.3	11
111	High-Utilisation Nanoplatinum Catalyst (Pt@cPIM) Obtained via Vacuum Carbonisation in a Molecularly Rigid Polymer of Intrinsic Microporosity. Electrocatalysis, 2017, 8, 132-143.	3.0	12
112	Potassium cation induced ionic diode blocking for a polymer of intrinsic microporosity nafion "heterojunction―on a microhole substrate. Electrochimica Acta, 2017, 258, 807-813.	5.2	21
113	Bacteriophages-Carbon Nanofibre Modified Electrodes for Biosensing Applications. Proceedings (mdpi), 2017, 1, .	0.2	0
114	Fabrication of a Horizontal and a Vertical Large Surface Area Nanogap Electrochemical Sensor. Sensors, 2016, 16, 2128.	3.8	8
115	Generatorâ€collector Voltammetry at Dualâ€plate Goldâ€gold Microtrench Electrodes as Diagnostic Tool in Ionic Liquids. Electroanalysis, 2016, 28, 1068-1076.	2.9	3
116	Residual Porosity of 3D‣AMâ€Printed Stainlessâ€Steel Electrodes Allows Galvanic Exchange Platinisation. ChemElectroChem, 2016, 3, 1020-1025.	3.4	7
117	Hydrodynamic Rocking Disc Electrode Study of the TEMPOâ€mediated Catalytic Oxidation of Primary Alcohols. Electroanalysis, 2016, 28, 2093-2103.	2.9	7
118	Estimation of Energy Levels of Self-assembled Ferrocenyls and Investigation of Charge-driven Electro-crystallization of Ferricenyl Materials. Energy Procedia, 2016, 100, 149-154.	1.8	3
119	Reagentless Electrochemiluminescence from a Nanoparticulate Polymer of Intrinsic Microporosity (PIMâ€1) Immobilized onto Tinâ€Doped Indium Oxide. ChemElectroChem, 2016, 3, 2160-2164.	3.4	7
120	Metal@MOF Materials in Electroanalysis: Silver-Enhanced Oxidation Reactivity Towards Nitrophenols Adsorbed into a Zinc Metal Organic Framework—Ag@MOF-5(Zn). Electrochimica Acta, 2016, 219, 482-491.	5.2	49
121	Hydrophobicity effects in iron polypyridyl complex electrocatalysis within Nafion thin-film electrodes. Physical Chemistry Chemical Physics, 2016, 18, 23365-23373.	2.8	4
122	Molecularly Rigid Microporous Polyamine Captures and Stabilizes Conducting Platinum Nanoparticle Networks. ACS Applied Materials & Interfaces, 2016, 8, 22425-22430.	8.0	14
123	Photoelectrocatalytic properties of BiVO4 prepared with different alcohol solvents. International Journal of Hydrogen Energy, 2016, 41, 17380-17389.	7.1	15
124	A Modular Bioplatform Based on a Versatile Supramolecular Multienzyme Complex Directly Attached to Graphene. ACS Applied Materials & Interfaces, 2016, 8, 21077-21088.	8.0	14
125	Modified Filamentous Bacteriophage as a Scaffold for Carbon Nanofiber. Bioconjugate Chemistry, 2016, 27, 2900-2910.	3.6	16
126	Allâ€Polystyrene 3Dâ€Printed Electrochemical Device with Embedded Carbon Nanofiberâ€Graphiteâ€Polystyrene Composite Conductor. Electroanalysis, 2016, 28, 1517-1523.	2.9	141

#	Article	IF	CITATIONS
127	pH-induced reversal of ionic diode polarity in 300 nm thin membranes based on a polymer of intrinsic microporosity. Electrochemistry Communications, 2016, 69, 41-45.	4.7	30
128	Nanostructured heated gold electrodes for DNA hybridization detection using enzyme labels. Sensors and Actuators B: Chemical, 2016, 233, 502-509.	7.8	5
129	Fuel cell anode catalyst performance can be stabilized with a molecularly rigid film of polymers of intrinsic microporosity (PIM). RSC Advances, 2016, 6, 9315-9319.	3.6	16
130	Theory of unsupported, steady-state, Nernstian, three-ion, twin-electrode, voltammetry: the special case of dual concentration polarization. Journal of Solid State Electrochemistry, 2016, 20, 3083-3095.	2.5	4
131	Synthesis and characterization of porous carbon–MoS ₂ nanohybrid materials: electrocatalytic performance towards selected biomolecules. Journal of Materials Chemistry B, 2016, 4, 1448-1457.	5.8	23
132	Ion flow in a zeolitic imidazolate framework results in ionic diode phenomena. Chemical Communications, 2016, 52, 2792-2794.	4.1	25
133	In situ microwave-enhanced electrochemical reactions at stainless steel: Nano-iron for aqueous pollutant degradation. Electrochemistry Communications, 2016, 62, 48-51.	4.7	7
134	Polymers of intrinsic microporosity in electrochemistry: Anion uptake and transport effects in thin film electrodes and in free-standing ionic diode membranes. Journal of Electroanalytical Chemistry, 2016, 779, 241-249.	3.8	21
135	An investigation of electrochemical contact processes for silver-wire glassy carbon and silver-coated cotton textile glassy carbon. New Journal of Chemistry, 2016, 40, 2814-2822.	2.8	6
136	Hydrodynamic Voltammetry at a Rocking Disc Electrode: Theory versus Experiment. Electrochimica Acta, 2016, 188, 837-844.	5.2	9
137	Polymer of Intrinsic Microporosity Induces Host-Guest Substrate Selectivity in Heterogeneous 4-Benzoyloxy-TEMPO-Catalysed Alcohol Oxidations. Electrocatalysis, 2016, 7, 70-78.	3.0	18
138	Photoanodes on titanium substrates: one-step deposited BiVO4 versus two-step nano-V2O5 films impregnated with Bi3+. Journal of Solid State Electrochemistry, 2016, 20, 273-283.	2.5	4
139	Carbon Microsphere – Polystyrene Composite Electrode for Threeâ€Phase Boundary Oil Analysis: Quinizarin in Methyllaurate. Electroanalysis, 2015, 27, 1043-1049.	2.9	0
140	ITOâ€ITO Dualâ€Plate Microgap Electrodes: E and EC′ Generatorâ€Collector Processes. Electroanalysis, 2015, 27, 1035-1042.	2.9	11
141	Microwire Chronoamperometric Determination of Concentration, Diffusivity, and Salinity for Simultaneous Oxygen and Proton Reduction. Electroanalysis, 2015, 27, 1829-1835.	2.9	12
142	Hydrodynamic Microgap Voltammetry under Couette Flow Conditions: Electrochemistry at a Rotating Drum in Viscous Poly(ethylene glycol). ChemPhysChem, 2015, 16, 2789-2796.	2.1	1
143	Boronâ€Doped Diamond Dualâ€Plate Deepâ€Microtrench Device for Generatorâ€Collector Sulfide Sensing. Electroanalysis, 2015, 27, 2645-2653.	2.9	6
144	Selective formation of hydrogen peroxide by oxygen reduction on TiO2 nanotubes in alkaline media. Electrochimica Acta, 2015, 174, 557-562.	5.2	25

#	Article	IF	CITATIONS
145	Feedbackâ€amplified electrochemical dualâ€plate boronâ€doped diamond microtrench detector for flow injection analysis. Electrophoresis, 2015, 36, 1866-1871.	2.4	3
146	Amplified electron transfer at poly-ethylene-glycol (PEG) grafted electrodes. Physical Chemistry Chemical Physics, 2015, 17, 11260-11268.	2.8	25
147	Chemoselective Oxidation of Sulfides to Sulfoxides with Urea–Hydrogen Peroxide Complex Catalysed by Diselenide. Synlett, 2015, 27, 80-82.	1.8	18
148	Pico-electrochemistry in humidity-equilibrated electrolyte films on nano-cotton: Three- and four-point probe voltammetry and impedance. Sensors and Actuators B: Chemical, 2015, 210, 762-767.	7.8	1
149	Electrocatalytic Carbohydrate Oxidation with 4-Benzoyloxy-TEMPO Heterogenised in a Polymer of Intrinsic Microporosity. Electrochimica Acta, 2015, 160, 195-201.	5.2	25
150	Aerosolâ€Assisted CVD of Bismuth Vanadate Thin Films and Their Photoelectrochemical Properties. Chemical Vapor Deposition, 2015, 21, 41-45.	1.3	55
151	Ferroceneâ€Boronic Acid–Fructose Binding Based on Dualâ€Plate Generator–Collector Voltammetry and Squareâ€Wave Voltammetry. ChemElectroChem, 2015, 2, 867-871.	3.4	6
152	Solid-solid EC' TEMPO-electrocatalytic conversion of diphenylcarbinol to benzophenone. Journal of Solid State Electrochemistry, 2015, 19, 1277-1283.	2.5	2
153	Intrinsically microporous polymer slows down fuel cell catalyst corrosion. Electrochemistry Communications, 2015, 59, 72-76.	4.7	28
154	Interfacial Electron-Shuttling Processes across KolliphorEL Monolayer Grafted Electrodes. ACS Applied Materials & Interfaces, 2015, 7, 15458-15465.	8.0	10
155	Water desalination concept using an ionic rectifier based on a polymer of intrinsic microporosity (PIM). Journal of Materials Chemistry A, 2015, 3, 15849-15853.	10.3	54
156	Sub-stoichiometric functionally graded titania fibres for water-splitting applications. Journal of Semiconductors, 2015, 36, 063001.	3.7	1
157	Mesoporous Nickel/Nickel Hydroxide Catalyst Using Liquid Crystal Template for Ethanol Oxidation in Alkaline Solution. Journal of the Electrochemical Society, 2015, 162, H453-H459.	2.9	31
158	Intrinsically Microporous Polymer Retains Porosity in Vacuum Thermolysis to Electroactive Heterocarbon. Langmuir, 2015, 31, 12300-12306.	3.5	25
159	New application for the BiVO4 photoanode: A photoelectroanalytical sensor for nitrite. Electrochemistry Communications, 2015, 61, 1-4.	4.7	45
160	Electrochemical sensing using boronic acids. Chemical Communications, 2015, 51, 14562-14573.	4.1	79
161	Polymers of intrinsic microporosity as high temperature templates for the formation of nanofibrous oxides. RSC Advances, 2015, 5, 73323-73326.	3.6	22
162	A redox-activated fluorescence switch based on a ferrocene–fluorophore–boronic ester conjugate. Chemical Communications, 2015, 51, 1293-1296.	4.1	55

#	Article	IF	CITATIONS
163	Nitrite/nitrate detection in serum based on dual-plate generator–collector currents in a microtrench. Talanta, 2015, 131, 228-235.	5.5	18
164	One-step preparation of the BiVO4 film photoelectrode. Journal of Solid State Electrochemistry, 2015, 19, 31-35.	2.5	24
165	Boron-doped diamond dual-plate microtrench electrode for generator–collector chloride/chlorine sensing. Electrochemistry Communications, 2014, 46, 120-123.	4.7	20
166	Oil Water Interfacial Phosphate Transfer Facilitated by Boronic Acid: Observation of Unusually Fast Oil Water Lateral Charge Transport. ChemElectroChem, 2014, 1, 1587-1587.	3.4	0
167	Intrinsically Porous Polymer Protects Catalytic Gold Particles for Enzymeless Glucose Oxidation. Electroanalysis, 2014, 26, 904-909.	2.9	39
168	Special Issue in Honour of Professor Stephen Fletcher. Journal of Solid State Electrochemistry, 2014, 18, 3215-3215.	2.5	0
169	"Roll-on―nano-CIGSe film electrodes in photo-hydrogenation. Journal of Photochemistry and Photobiology A: Chemistry, 2014, 276, 65-70.	3.9	1
170	Functionalized Carbon Nanoparticles, Blacks and Soots as Electronâ€Transfer Building Blocks and Conduits. Chemistry - an Asian Journal, 2014, 9, 1226-1241.	3.3	39
171	Nano-Litre Proton/Hydrogen Titration in a Dual-Plate Platinum-Platinum Generator-Collector Electrode Micro-Trench. Electrochimica Acta, 2014, 125, 94-100.	5.2	19
172	A dual-plate ITO–ITO generator–collector microtrench sensor: surface activation, spatial separation and suppression of irreversible oxygen and ascorbate interference. Analyst, The, 2014, 139, 569-575.	3.5	25
173	Voltammetric optimisation of TEMPO-mediated oxidations at cellulose fabric. Green Chemistry, 2014, 16, 3322-3327.	9.0	29
174	Electrochemical determination of selected neurotransmitters at electrodes modified with oppositely charged carbon nanoparticles. Analytical Methods, 2014, 6, 7532-7539.	2.7	14
175	Cavity transport effects in generator–collector electrochemical analysis of nitrobenzene. Physical Chemistry Chemical Physics, 2014, 16, 18966-18973.	2.8	9
176	Hydrothermal Conversion of One-Photon-Fluorescent Poly(4-vinylpyridine) into Two-Photon-Fluorescent Carbon Nanodots. Langmuir, 2014, 30, 11746-11752.	3.5	24
177	Oil Water Interfacial Phosphate Transfer Facilitated by Boronic Acid: Observation of Unusually Fast Oil Water Lateral Charge Transport. ChemElectroChem, 2014, 1, 1640-1646.	3.4	11
178	Detection and Characterization of Liquid Solid and Liquid Liquid Solid Interfacial Gradients of Water Nanodroplets in Wet <i>N</i> -Octyl-2-Pyrrolidone. Langmuir, 2014, 30, 9951-9961.	3.5	8
179	Cysteine-Cystine Redox Cycling in a Gold–Gold Dual-Plate Generator-Collector Microtrench Sensor. Analytical Chemistry, 2014, 86, 6748-6752.	6.5	26
180	Metastable Ionic Diodes Derived from an Amineâ€Based Polymer of Intrinsic Microporosity. Angewandte Chemie - International Edition, 2014, 53, 10751-10754.	13.8	81

#	Article	IF	CITATIONS
181	Ionâ€Transfer Voltammetry at Carbon Nanofibre Membranes Produced by 500 °C Graphitisation/Graphenisation of Electrospun Polyâ€Acrylonitrile. Electroanalysis, 2014, 26, 69-75.	2.9	2
182	Liquid Liquid Interfacial Photoelectrochemistry of Chromoionophoreâ€I Immobilised in 4â€(3â€Phenylpropyl)Pyridine Microdroplets. ChemElectroChem, 2014, 1, 400-406.	3.4	2
183	Mass transport and modulation effects in rocking dual-semi-disc electrode voltammetry. Journal of Electroanalytical Chemistry, 2014, 722-723, 78-82.	3.8	8
184	New di-ferrocenyl-ethynylpyridinyl triphenylphosphine copper halide complexes and related di-ferricenyl electro-crystallized materials. Dalton Transactions, 2014, 43, 9497-9507.	3.3	9
185	High density heterogenisation of molecular electrocatalysts in a rigid intrinsically microporous polymer host. Electrochemistry Communications, 2014, 46, 26-29.	4.7	28
186	Polymers of intrinsic microporosity in electrocatalysis: Novel pore rigidity effects and lamella palladium growth. Electrochimica Acta, 2014, 128, 3-9.	5.2	42
187	One-step electroless growth of nano-fibrous platinum catalyst from "paint-on―PtCl62- solution in poly-(ethylene-glycol). Electrochimica Acta, 2014, 137, 484-488.	5.2	7
188	Electrochemical Microflow Systems. , 2014, , 516-522.		0
189	Photoelectrochemical Transients for Chlorine/Hypochlorite Formation at "Roll-On― Nano-WO ₃ Film Electrodes. Journal of Physical Chemistry C, 2013, 117, 7005-7012.	3.1	25
190	Pyrene-anchored boronic acid receptors on carbon nanoparticle supports: fluxionality and pore effects. New Journal of Chemistry, 2013, 37, 1883.	2.8	18
191	A gold–gold oil microtrench electrode for liquid–liquid anion transfer voltammetry. Electrophoresis, 2013, 34, 1979-1984.	2.4	11
192	Selfâ€Assembled Regenerated Cellulose Spacer Film in Thin Film and Generatorâ€Collector Electrodes. Electroanalysis, 2013, 25, 1773-1779.	2.9	2
193	Formation of low density hydrous iron oxide via conformal transformation of MIL-53(Fe). Chemical Communications, 2013, 49, 10593.	4.1	3
194	New Multi-Ferrocenyl- and Multi-Ferricenyl- Materials via Coordination-Driven Self-Assembly and via Charge-Driven Electro-Crystallization. Inorganic Chemistry, 2013, 52, 12012-12022.	4.0	11
195	"Hydrothermal wrapping―with poly(4-vinylpyridine) introduces functionality: pH-sensitive core–shell carbon nanomaterials. Journal of Materials Chemistry A, 2013, 1, 4559.	10.3	6
196	Pulse electroanalysis at gold–gold micro-trench electrodes: Chemical signal filtering. Faraday Discussions, 2013, 164, 349.	3.2	10
197	Exploiting the Reversible Covalent Bonding of Boronic Acids: Recognition, Sensing, and Assembly. Accounts of Chemical Research, 2013, 46, 312-326.	15.6	559
198	Crystal growth of Cu2ZnSnS4 solar cell absorber by chemical vapor transport with I2. Journal of Crystal Growth, 2013, 364, 101-110.	1.5	25

#	Article	IF	CITATIONS
199	Proton uptake vs. redox driven release from metal–organic-frameworks: Alizarin red S reactivity in UMCM-1. Journal of Electroanalytical Chemistry, 2013, 689, 168-175.	3.8	17
200	Carbon nanoparticulate films as effective scaffolds for mediatorless bioelectrocatalytic hydrogen oxidation. Electrochimica Acta, 2013, 111, 434-440.	5.2	11
201	Reprint of proton uptake vs. redox driven release from metal–organic-frameworks: Alizarin red S reactivity in UMCM-1. Journal of Electroanalytical Chemistry, 2013, 710, 2-9.	3.8	3
202	Dual band electrodes in generator–collector mode: Simultaneous measurement of two species. Journal of Electroanalytical Chemistry, 2013, 703, 38-44.	3.8	15
203	Hydrogen Peroxide Detection in Wet Air with a Prussian Blue Based Solid Salt Bridged Three Electrode System. Analytical Chemistry, 2013, 85, 2574-2577.	6.5	16
204	Long-Range Intramolecular Electronic Communication in Bis(ferrocenylethynyl) Complexes Incorporating Conjugated Heterocyclic Spacers: Synthesis, Crystallography, and Electrochemistry. Inorganic Chemistry, 2013, 52, 4898-4908.	4.0	24
205	Plasmon Resonance Scattering Spectroscopy at the Singleâ€Nanoparticle Level: Realâ€Time Monitoring of a Click Reaction. Angewandte Chemie - International Edition, 2013, 52, 6011-6014.	13.8	178
206	Imparting pH- and small molecule selectivity to nano-Pd catalysts via hydrothermal wrapping with chitosan. Electrochimica Acta, 2013, 110, 663-669.	5.2	5
207	Generator–collector electroanalysis at tin-doped indium oxide–epoxy–tin-doped indium oxide junction electrodes. Electrochimica Acta, 2013, 101, 196-200.	5.2	10
208	Direct electrochemistry of adsorbed proteins and bioelectrocatalysis at film electrode prepared from oppositely charged carbon nanoparticles. Electrochimica Acta, 2013, 89, 132-138.	5.2	17
209	Conformal transformation of [Co(bdc)(DMF)] (Co-MOF-71, bdc = 1,4-benzenedicarboxylate, DMF =) Tj ETQq1 1 Communications, 2013, 27, 9-13.	0.784314 4.7	rgBT /Overlo 121
210	Interdigitated ring electrodes: Theory and experiment. Journal of Electroanalytical Chemistry, 2013, 709, 57-64.	3.8	10
211	"Indirect Modification―of Glassy Carbon with Gold Nanoparticles Using Nonconducting Support Materials. Electroanalysis, 2013, 25, 975-982.	2.9	7
212	Highly Sensitive Junction Electrodes with Self-Assembled Regenerated Cellulose Thin Films. ECS Meeting Abstracts, 2013, , .	0.0	0
213	Redox Reactivity of Methylene Blue Bound in Pores of UMCM-1 Metal-Organic Frameworks. Molecular Crystals and Liquid Crystals, 2012, 554, 12-21.	0.9	7
214	Surface State Trapping and Mobility Revealed by Junction Electrochemistry of Nano-Cr2O3. Australian Journal of Chemistry, 2012, 65, 65.	0.9	13
215	Simplest Prussian-blue deposition from ferric ferricyanide solution by a reducing Ag spot put onto an ITO substrate. Journal of Solid State Electrochemistry, 2012, 16, 3723-3724.	2.5	3
216	Harnessing applied potential to oxidation in water. Green Chemistry, 2012, 14, 2221.	9.0	19

#	Article	IF	CITATIONS
217	DEMS-monitoring liquid gas interfacial ammonia oxidation at carbon nanofibre membranes. RSC Advances, 2012, 2, 4886.	3.6	5
218	Cellulose Nanowhiskers in Electrochemical Applications. ACS Symposium Series, 2012, , 75-106.	0.5	11
219	Metal–organic frameworks post-synthetically modified with ferrocenyl groups: framework effects on redox processes and surface conduction. Dalton Transactions, 2012, 41, 1475-1480.	3.3	57
220	Inter-particle charge transfer in TiO2-phytate films: Generator–collector gold–gold junction transients. Journal of Electroanalytical Chemistry, 2012, 686, 32-37.	3.8	6
221	Rocking disc electro-deposition of CuIn alloys, selenisation, and pinhole effect minimisation in CISe solar absorber layers. Electrochimica Acta, 2012, 79, 141-147.	5.2	14
222	New Insights into Water Splitting at Mesoporous α-Fe ₂ O ₃ Films: A Study by Modulated Transmittance and Impedance Spectroscopies. Journal of the American Chemical Society, 2012, 134, 1228-1234.	13.7	162
223	Ferrocene-Decorated Nanocrystalline Cellulose with Charge Carrier Mobility. Langmuir, 2012, 28, 6514-6519.	3.5	63
224	Hydrothermal core–shell carbon nanoparticle films: thinning the shell leads to dramatic pH response. Physical Chemistry Chemical Physics, 2012, 14, 15860.	2.8	9
225	Decamethylferrocene Redox Chemistry and Gold Nanowire Electrodeposition at Salt Crystal Electrode Nonpolar Organic Solvent Contacts. Organometallics, 2012, 31, 2616-2620.	2.3	1
226	Generator-collector double electrode systems: A review. Analyst, The, 2012, 137, 1068.	3.5	98
227	Kinetics and mechanism of light-driven oxygen evolution at thin film α-Fe2O3 electrodes. Chemical Communications, 2012, 48, 2027.	4.1	207
228	Coil-by-coil assembly of poly[acrylamide-co-3-(methacryl-amido)-phenylboronic acid] with polydiallyldimethyl-ammonium to give alizarin red S responsive films. Journal of Materials Chemistry, 2012, 22, 18999.	6.7	8
229	Goldâ€gold junction electrodes:the disconnection method. Chemical Record, 2012, 12, 143-148.	5.8	11
230	The Development of Boronic Acids as Sensors and Separation Tools. Chemical Record, 2012, 12, 464-478.	5.8	61
231	Microwave Activation of Electrochemical Processes in Ionic Liquid Impregnated Ionomer Spheres. Electroanalysis, 2012, 24, 997-1002.	2.9	1
232	Dioctylamineâ€ S ulfonamideâ€Modified Carbon Nanoparticles as High Surface Area Substrates for Coenzyme Q10Lipid Electrochemistry. Electroanalysis, 2012, 24, 1003-1010.	2.9	11
233	Mesoporous Silica Sputterâ€Coated onto ITO: Electrochemical Processes, Ion Permeability, and Gold Deposition Through NanoPores. Electroanalysis, 2012, 24, 1296-1305.	2.9	5
234	Chitosanâ€Based Hydrothermal Nanocarbon: Coreâ€Shell Characteristics and Composite Electrodes. Electroanalysis, 2012, 24, 1703-1708.	2.9	6

#	Article	IF	CITATIONS
235	Square Wave Electroanalysis at Generator–Collector Gold–Gold Double Hemisphere Junctions. Electroanalysis, 2012, 24, 1726-1731.	2.9	5
236	Suppressed photoelectrochemistry at carbon-surface-modified mesoporous TiO2 films. Electrochimica Acta, 2012, 73, 31-35.	5.2	8
237	Voltammetric probing of pH at carbon nanofiber–Nafion™–carbon nanofiber membrane electrode assemblies. Electrochimica Acta, 2012, 62, 97-102.	5.2	9
238	Nano-TiO2-flavin adenine dinucleotide film redox processes in contact to humidified gas salt electrolyte. Bioelectrochemistry, 2012, 86, 54-59.	4.6	1
239	Surface-dopylated carbon nanoparticles sense gas-induced pH changes. Sensors and Actuators B: Chemical, 2012, 161, 184-190.	7.8	9
240	Carbon nanoparticle–chitosan composite electrode with anion, cation, and neutral binding sites: Dihydroxybenzene selectivity. Sensors and Actuators B: Chemical, 2012, 162, 194-200.	7.8	45
241	Mechanistic aspects of aldehyde and imine electro-reduction in a liquid–liquid carbon nanofiber membrane microreactor. Tetrahedron Letters, 2012, 53, 3357-3360.	1.4	10
242	Spectroelectrochemical Investigation of TPPMn(III/II)â€Driven Liquid Liquid Electrode Triple Phase Boundary Anion Transfer into 4â€(3â€Phenylpropyl)â€Pyridine: ClO ₄ ^{â^'} , CO ₃ H ^{â^'} , Cl ^{â^'} , and F ^{â^'} . Electroanalysis, 2012, 24, 246-253.	2.9	9
243	Ion-transfer- and photo-electrochemistry at liquid liquid solid electrode triple phase boundary junctions: perspectives. Physical Chemistry Chemical Physics, 2011, 13, 10036.	2.8	32
244	Enhanced TiO2 surface electrochemistry with carbonised layer-by-layer cellulose-PDDA composite films. Physical Chemistry Chemical Physics, 2011, 13, 9857.	2.8	8
245	Liquid Liquid Electrode Triple-Phase Boundary Photovoltammetry of Pentoxyresorufin in 4-(3-Phenylpropyl)pyridine. Langmuir, 2011, 27, 6471-6477.	3.5	7
246	The Synucleins Are a Family of Redox-Active Copper Binding Proteins. Biochemistry, 2011, 50, 37-47.	2.5	66
247	Contribution of Individual Histidines to Prion Protein Copper Binding. Biochemistry, 2011, 50, 10781-10791.	2.5	21
248	Liquid liquid electrochemical bicarbonate and carbonate capture facilitated by boronic acids. Chemical Communications, 2011, 47, 12002.	4.1	10
249	Electrode processes at gas salt Pd nanoparticle glassy carbon electrode contacts: salt effects on the oxidation of formic acid vapor and the oxidation of hydrogen. New Journal of Chemistry, 2011, 35, 1855.	2.8	9
250	Nanoparticles in electrochemical sensors for environmental monitoring. TrAC - Trends in Analytical Chemistry, 2011, 30, 1704-1715.	11.4	231
251	Rocking disc electro-deposition of copper films on Mo/MoSe2 substrates. Thin Solid Films, 2011, 519, 7458-7463.	1.8	5
252	Tuning percolation speed in layer-by-layer assembled polyaniline–nanocellulose composite films. Journal of Solid State Electrochemistry, 2011, 15, 2675-2681.	2.5	24

#	Article	IF	CITATIONS
253	Carbon Nanoparticle Surface Electrochemistry: Highâ€Density Covalent Immobilisation and Poreâ€Reactivity of 9,10â€Anthraquinone. Electroanalysis, 2011, 23, 1320-1324.	2.9	22
254	Electroanalysis at Salt – Cotton – Electrode Interfaces: Preconcentration Effects Lead to Nanoâ€Molar Hg ²⁺ Sensitivity. Electroanalysis, 2011, 23, 2149-2155.	2.9	6
255	Paper supports in electrocatalysis: Weak contact catalysis with seed-mediated grown gold nanoparticle deposits. Electrochemistry Communications, 2011, 13, 68-71.	4.7	5
256	Salt matrix voltammetry: Microphase redox processes at ammonium chloride gold gas triple phase boundaries. Electrochemistry Communications, 2011, 13, 154-157.	4.7	10
257	Liquid–liquid electro-organo-synthetic processes in a carbon nanofibre membrane microreactor: Triple phase boundary effects in the absence of intentionally added electrolyte. Electrochimica Acta, 2011, 56, 6764-6770.	5.2	10
258	Dual-microdisk electrodes in transient generator–collector mode: Experiment and theory. Journal of Electroanalytical Chemistry, 2011, 655, 147-153.	3.8	16
259	Electron hopping rate measurements in ITO junctions: Charge diffusion in a layer-by-layer deposited ruthenium(II)-bis(benzimidazolyI)pyridine-phosphonate–TiO2 film. Journal of Electroanalytical Chemistry, 2011, 657, 196-201.	3.8	13
260	Assembly of N-hexadecyl-pyridinium-4-boronic acid hexafluorophosphate monolayer films with catechol sensing selectivity. Journal of Materials Chemistry, 2010, 20, 8305.	6.7	60
261	Boronic aciddendrimerreceptor modified nanofibrillar cellulose membranes. Journal of Materials Chemistry, 2010, 20, 588-594.	6.7	37
262	Microwave-electrochemical formation of colloidal zinc oxide at fluorine doped tin oxide electrodes. Electrochimica Acta, 2010, 55, 7909-7915.	5.2	10
263	CuInSe2 precursor films electro-deposited directly onto MoSe2. Journal of Electroanalytical Chemistry, 2010, 645, 16-21.	3.8	8
264	Adsorption and redox chemistry of cis-RuLL'(SCN)2 with L=4,4′-dicarboxylic acid-2,2′-bipyridine and L'=4,4′-dinonyl-2,2′-bipyridine (Z907) at FTO and TiO2 electrode surfaces. Journal of Solid State Electrochemistry, 2010, 14, 1929-1936.	2.5	23
265	dsDNA modified carbon nanofiber—solidified paste electrodes: probing Ni(II)—dsDNA interactions. Mikrochimica Acta, 2010, 170, 155-164.	5.0	9
266	Triple Phase Boundary Photovoltammetry: Resolving Rhodamine B Reactivity in 4â€(3â€Phenylpropyl)â€Pyridine Microdroplets. ChemPhysChem, 2010, 11, 2862-2870.	2.1	11
267	Ultrathin Carbon Film Electrodes from Vacuumâ€Carbonised Cellulose Nanofibril Composite. Electroanalysis, 2010, 22, 619-624.	2.9	19
268	Ion Transport Across Liquid Liquid Interfacial Boundaries Monitored at Generator ollector Electrodes. Electroanalysis, 2010, 22, 2889-2896.	2.9	10
269	Cis-bis(isothiocyanato)-bis(2,2′-bipyridyl-4,4′dicarboxylato)-Ru(II) (N719) dark-reactivity when bound to fluorine-doped tin oxide (FTO) or titanium dioxide (TiO2) surfaces. Journal of Electroanalytical Chemistry, 2010, 640, 61-67.	3.8	18
270	An ambient aqueous synthesis for highly dispersed and active Pd/C catalyst for formic acid electro-oxidation. Journal of Power Sources, 2010, 195, 7246-7249.	7.8	80

#	Article	IF	CITATIONS
271	Active catalysts of sonoelectrochemically prepared iron metal nanoparticles for the electroreduction of chloroacetates. Physics Procedia, 2010, 3, 105-109.	1.2	3
272	Coupled triple phase boundary processes: Liquid–liquid generator–collector electrodes. Electrochemistry Communications, 2010, 12, 455-458.	4.7	8
273	Three dimensional film electrode prepared from oppositely charged carbon nanoparticles as efficient enzyme host. Electrochemistry Communications, 2010, 12, 737-739.	4.7	34
274	Facile cation electro-insertion into layer-by-layer assembled iron phytate films. Electrochemistry Communications, 2010, 12, 1722-1726.	4.7	8
275	One-step growth of 3–5nm diameter palladium electrocatalyst in a carbon nanoparticle–chitosan host and characterization for formic acid oxidation. Electrochimica Acta, 2010, 55, 6601-6610.	5.2	37
276	Liquid liquid biphasic electrochemistry in ultra-turrax dispersed acetonitrile aqueous electrolyte systems. Electrochimica Acta, 2010, 55, 8808-8814.	5.2	15
277	Nanostructured electrodes for biocompatible CMOS integrated circuits. Sensors and Actuators B: Chemical, 2010, 147, 697-706.	7.8	11
278	Electrocatalytic activity of BasoliteTM F300 metal-organic-framework structures. Electrochemistry Communications, 2010, 12, 632-635.	4.7	99
279	UV/Vis/NIR Spectroelectrochemistry. , 2010, , 179-200.		3
280	Carbon nanoparticle surface functionalisation: converting negatively charged sulfonate to positively charged sulfonamide. Physical Chemistry Chemical Physics, 2010, 12, 4872.	2.8	27
281	Fast Hole Surface Conduction Observed for Indoline Sensitizer Dyes Immobilized at Fluorine-Doped Tin Oxideâ°'TiO2 Surfaces. Journal of Physical Chemistry C, 2010, 114, 11822-11828.	3.1	41
282	Discharge cavitation during microwave electrochemistry at micrometre-sized electrodes. Chemical Communications, 2010, 46, 812-814.	4.1	10
283	Pulse-Voltammetric Glucose Detection at Gold Junction Electrodes. Analytical Chemistry, 2010, 82, 7063-7067.	6.5	40
284	Solvent-Dependent Changes in Molecular Reorientation Dynamics: The Role of Solventâ^'Solvent Interactions. Journal of Physical Chemistry A, 2010, 114, 4957-4962.	2.5	16
285	Effects of Electrolyte Concentration on the Rotational Dynamics of Resorufin. Journal of Physical Chemistry A, 2010, 114, 12875-12880.	2.5	4
286	Cyclic Voltammetry. , 2010, , 57-106.		28
287	N,N-Butyl-decamethylferrocenyl-amine reactivity at liquid liquid interfaces: electrochemically driven anion transfer vs. pH driven proton transfer. New Journal of Chemistry, 2010, 34, 1261.	2.8	10
288	Screening Anti-Oxidant Activity at Oil Microdroplet Triple Phase Boundary Electrodes. , 2009, , .		0

17

#	Article	IF	CITATIONS
289	Nanomechanical electron shuttle consisting of a gold nanoparticle embedded within the gap between two gold electrodes. Physical Review B, 2009, 79, .	3.2	37
290	Fabrication of shuttle-junctions for nanomechanical transfer of electrons. Nanotechnology, 2009, 20, 485202.	2.6	10
291	Electrochemically Active Mercury Nanodroplets Trapped in a Carbon Nanoparticle–Chitosan Matrix. Electroanalysis, 2009, 21, 261-266.	2.9	21
292	Probing Second Harmonic Components of pHâ€Sensitive Redox Processes in a Mesoporous TiO ₂ â€Nafion Film Electrode with Fourierâ€Transformed Largeâ€Amplitude Sinusoidally Modulated Voltammetry. Electroanalysis, 2009, 21, 41-47.	2.9	7
293	Microwaveâ€Assisted Electroanalysis: A Review. Electroanalysis, 2009, 21, 113-123.	2.9	38
294	Voltammetric Antioxidant Analysis in Mineral Oil Samples Immobilized into Boronâ€Đoped Diamond Micropore Array Electrodes. Electroanalysis, 2009, 21, 1341-1347.	2.9	7
295	Liquid–liquid ion transport junctions based on paired gold electrodes in generator–collector mode. Electrophoresis, 2009, 30, 3361-3365.	2.4	12
296	Growth and characterisation of diffusion junctions between paired gold electrodes: diffusion effects in generator–collector mode. Journal of Solid State Electrochemistry, 2009, 13, 609-617.	2.5	18
297	Boronic acid-facilitated α-hydroxy-carboxylate anion transfer at liquid/liquid electrode systems: the ElCrev mechanism. Journal of Solid State Electrochemistry, 2009, 13, 1475-1482.	2.5	28
298	Twoâ€phase flow electrosynthesis: Comparing <i>N</i> â€octylâ€2â€pyrrolidone–aqueous and acetonitrile–aqueous threeâ€phase boundary reactions. Journal of Physical Organic Chemistry, 2009, 22, 52-58.	1.9	26
299	Paired gold junction electrodes with submicrometer gap. Journal of Electroanalytical Chemistry, 2009, 632, 206-210.	3.8	20
300	Aqueous-organic biphasic redox-chemistry of high-hydride content rhodium clusters: Towards immobilisation of redox-switchable H2 binding materials on a surface. Journal of Organometallic Chemistry, 2009, 694, 2808-2813.	1.8	4
301	Hydrophilic carbon nanoparticle-laccase thin film electrode for mediatorless dioxygen reduction. Electrochimica Acta, 2009, 54, 4620-4625.	5.2	66
302	Effects of microwave radiation on electrodeposition processes at tin-doped indium oxide (ITO) electrodes. Electrochimica Acta, 2009, 54, 6680-6685.	5.2	12
303	High-yield acetonitrile water triple phase boundary electrolysis at platinised Teflon electrodes. Electrochimica Acta, 2009, 54, 6908-6912.	5.2	8
304	Synthesis, Characterization, and Electrochemistry of a Series of Iron(II) Complexes Containing Self-Assembled 1,5-Diaza-3,7-diphosphabicyclo[3.3.1]nonane Ligands. Inorganic Chemistry, 2009, 48, 9924-9935.	4.0	8
305	Ultrasound Mobilization of Liquid/Liquid/Solid Triple-Phase Boundary Redox Systems. Journal of Physical Chemistry C, 2009, 113, 15629-15633.	3.1	10
306	Thermodynamic and Voltammetric Characterization of the Metal Binding to the Prion Protein: Insights into pH Dependence and Redox Chemistry. Biochemistry, 2009, 48, 2610-2619.	2.5	53

#	Article	IF	CITATIONS
307	Microwave-Enhanced Electrochemistry in Locally Superheated Aqueousâ^'Glycerol Electrolyte Media. Journal of Physical Chemistry C, 2009, 113, 3046-3049.	3.1	15
308	Anthraquinone catalysis in the glucose-driven reduction of indigo to leuco-indigo. Physical Chemistry Chemical Physics, 2009, 11, 1816.	2.8	22
309	Microwave-enhanced electroanalytical processes: generator–collector voltammetry at paired gold electrode junctions. Analyst, The, 2009, 134, 887.	3.5	15
310	Bioelectrocatalytic dioxygen reduction at hybrid silicate–polyallylamine film with encapsulated laccase. Journal of Electroanalytical Chemistry, 2008, 612, 1-8.	3.8	16
311	Sol–gel processed ionic liquid – hydrophilic carbon nanoparticles multilayer film electrode prepared by layer-by-layer method. Journal of Electroanalytical Chemistry, 2008, 623, 170-176.	3.8	36
312	Electrochemical and sonoelectrochemical monitoring of indigo reduction by glucose. Dyes and Pigments, 2008, 76, 542-549.	3.7	54
313	Assembly, conductivity, and chemical reactivity of sub-monolayer gold nanoparticle junction arrays. Sensors and Actuators B: Chemical, 2008, 129, 947-952.	7.8	12
314	Electrochemical determination of plant-derived leuco-indigo after chemical reduction by glucose. Journal of Applied Electrochemistry, 2008, 38, 1683-1690.	2.9	18
315	Introducing hydrophilic carbon nanoparticles into hydrophilic sol-gel film electrodes. Journal of Solid State Electrochemistry, 2008, 12, 287-293 Layer-by-layer assembly of Ru3+ and % MathType!Translator!2!1!AMS LaTeX.tdl!TeX AMS-LaTeX! %	2.5	34
316	MathType!MTEF!2!1!+- % feaaeaart1ev0aqatCvAUfeBSjuyZL2yd9gzLbvyNv2CaerbuLwBLn % hiov2DGi1BTfMBaeXatLxBI9gBaerbd9wDYLwzYbItLDharqqtubsr % 4rNCHbGeaGqiVu0Je9sqqrpepC0xbbL8F4rqqrFfpeea0xe9Lq-Jc9 % vqaqpepm0xbba9pwe9Q8fs0-yqaqpepae9pg0FirpepeKkFr0xfr-x %	2.5	5
317	fr-xb9adbaqaaeGaciGaaiaabeqaamaabaabaaGcbaGaae4uaiaabM % gadaWgaaWchaGzaeioaaqabaGcccaaGpb Underpotential sufface reduction of mesoporous CeO2 nanoparticle films. Journal of Solid State Electrochemistry, 2008, 12, 1541-1548.	2.5	7
318	Electrocatalytic Determination of Sulfite at Immobilized Microdroplet Liquid∣Liquid Interfaces: The ElC′ Mechanism. Electroanalysis, 2008, 20, 469-475.	2.9	9
319	Arsenite Determination in Phosphate Media at Electroaggregated Gold Nanoparticle Deposits. Electroanalysis, 2008, 20, 1286-1292.	2.9	68
320	Nanofibrillar Celluloseâ€Chitosan Composite Film Electrodes: Competitive Binding of Triclosan, Fe(CN) ₆ ^{3â^'/4â^'} , and SDS Surfactant. Electroanalysis, 2008, 20, 2395-2402.	2.9	17
321	Growth and Application of Paired Gold Electrode Junctions: Evidence for Nitrosonium Phosphate During Nitric Oxide Oxidation. Electroanalysis, 2008, 20, 2403-2409.	2.9	31
322	Enantioselective Organocatalytic Epoxidation Driven by Electrochemically Generated Percarbonate and Persulfate. Advanced Synthesis and Catalysis, 2008, 350, 1149-1154.	4.3	61
323	Modified carbon nanoparticle-chitosan film electrodes: Physisorption versus chemisorption. Electrochimica Acta, 2008, 53, 5732-5738.	5.2	42
324	Chemically surface-modified carbon nanoparticle carrier for phenolic pollutants: Extraction and electrochemical determination of benzophenone-3 and triclosan. Analytica Chimica Acta, 2008, 616, 28-35.	5.4	64

#	Article	IF	CITATIONS
325	Electrochemically promoted Friedel–Crafts acylation of aromatic compounds. Tetrahedron Letters, 2008, 49, 2625-2627.	1.4	4
326	Reactivity of methemoglobin immobilized on TiO2 nanoparticle films. Bioelectrochemistry, 2008, 72, 1-2.	4.6	5
327	Direct reversible voltammetry and electrocatalysis with surface-stabilised Fe2O3 redox states. Electrochemistry Communications, 2008, 10, 1773-1776.	4.7	38
328	Fluorescent Boron Bis(phenolate) with Association Response to Chloride and Dissociation Response to Fluoride. Inorganic Chemistry, 2008, 47, 6236-6244.	4.0	42
329	Thin-Film Modified Electrodes with Reconstituted Celluloseâ `PDDAC Films for the Accumulation and Detection of Triclosan. Journal of Physical Chemistry C, 2008, 112, 2660-2666.	3.1	56
330	Chemical and electro-chemical applications of in situ microwave heating. Annual Reports on the Progress of Chemistry Section C, 2008, 104, 124.	4.4	15
331	Binding site control in a layer-by-layer deposited chitosan–carbon nanoparticle film electrode. New Journal of Chemistry, 2008, 32, 1253.	2.8	20
332	Optical waveguide spectroscopy study of the transport and binding of cytochrome c in mesoporous titanium dioxide electrodes Journal of Materials Chemistry, 2008, 18, 4304.	6.7	21
333	Probing carboxylate Gibbs transfer energies via liquid liquid transfer at triple phase boundary electrodes: ion-transfer voltammetry versus COSMO-RS predictions. Physical Chemistry Chemical Physics, 2008, 10, 3925.	2.8	34
334	Manganese Binding to the Prion Protein. Journal of Biological Chemistry, 2008, 283, 12831-12839.	3.4	90
335	The chemistry of thiophene S-oxides1 and related compounds. Arkivoc, 2008, 2009, 96-113.	0.5	3
336	Microwave-enhanced electro-deposition and stripping of palladium at boron-doped diamond electrodes. Talanta, 2007, 72, 66-71.	5.5	17
337	Sequential Reduction of High Hydride Count Octahedral Rhodium Clusters [Rh6(PR3)6H12][BArF4]2:Â Redox-Switchable Hydrogen Storage. Journal of the American Chemical Society, 2007, 129, 1793-1804.	13.7	37
338	Scaling out of electrolyte free electrosynthesis in a micro-gap flow cell. Lab on A Chip, 2007, 7, 141-143.	6.0	26
339	Voltammetric Measurements at the Surface of Cotton:Â Absorption and Catalase Reactivity of a Dinuclear Manganese Complex. Langmuir, 2007, 23, 2239-2246.	3.5	8
340	A New Method of Studying Ion Transfer at Liquid Liquid Phase Boundaries Using a Carbon Nanotube Paste Electrode with a Redox Active Binder. Journal of Physical Chemistry C, 2007, 111, 18353-18360.	3.1	13
341	Electrochemical Investigation of Hemispherical Microdroplets ofN,N-Didodecyl-N',N'-diethylphenylenediamine Immobilized as Regular Arrays on Partially-Blocked Electrodes:  A New Approach to Liquid Liquid Voltammetry. Journal of Physical Chemistry C, 2007, 111, 9992-10002.	3.1	31
342	Electrosynthesis of phenyl-2-propanone derivatives from benzyl bromides and acetic anhydride in an unsupported micro-flow cell electrolysis process. Green Chemistry, 2007, 9, 20-22.	9.0	22

#	Article	IF	CITATIONS
343	A Porous ITO Nanoparticles Modified Electrode for the Redox Liquid Immobilization. Electroanalysis, 2007, 19, 155-160.	2.9	23
344	Ultrathin Carbon Nanoparticle Composite Film Electrodes: Distinguishing Dopamine and Ascorbate. Electroanalysis, 2007, 19, 1032-1038.	2.9	67
345	Carbon Nanofiber–Polystyrene Composite Electrodes for Electroanalytical Processes. Electroanalysis, 2007, 19, 1461-1466.	2.9	27
346	Electro-deposition of thin cellulose films at boron-doped diamond substrates. Electrochemistry Communications, 2007, 9, 42-48.	4.7	10
347	Electrocatalytic oxidation of nitric oxide at TiO2–Au nanocomposite film electrodes. Electrochemistry Communications, 2007, 9, 436-442.	4.7	64
348	Electro-deposition and stripping of catalytically active iron metal nanoparticles at boron-doped diamond electrodes. Electrochemistry Communications, 2007, 9, 1127-1133.	4.7	22
349	Demetallation of methemoglobin in cellulose nanofibril–TiO2 nanoparticle composite membrane electrodes. Electrochemistry Communications, 2007, 9, 1985-1990.	4.7	30
350	Microwave activation of electrochemical processes: High temperature phenol and triclosan electro-oxidation at carbon and diamond electrodes. Electrochimica Acta, 2007, 53, 1092-1099.	5.2	38
351	Carbon nanoparticle stabilised liquid liquid micro-interfaces for electrochemically driven ion-transfer processes. Electrochimica Acta, 2007, 53, 1175-1181.	5.2	25
352	An ionic liquid as a solvent for headspace single drop microextraction of chlorobenzenes from water samples. Analytica Chimica Acta, 2007, 584, 189-195.	5.4	161
353	Electrostatic accumulation and determination of triclosan in ultrathin carbon nanoparticle composite film electrodes. Analytica Chimica Acta, 2007, 593, 117-122.	5.4	72
354	The effects of conductivity and electrochemical doping on the reduction of methemoglobin immobilized in nanoparticulate TiO2 films. Bioelectrochemistry, 2007, 70, 221-227.	4.6	19
355	Electrochemical processes at a flowing organic solventâ^£aqueous electrolyte phase boundary. Electrochemistry Communications, 2007, 9, 2105-2110.	4.7	33
356	Voltammetric study of absorption and reactivity of metal complexes in cotton immersed in aqueous buffer solutions. Journal of Electroanalytical Chemistry, 2007, 601, 211-219.	3.8	5
357	Boron-doped diamond electrodes in organic media: Electrochemical activation and selectivity effects. Journal of Electroanalytical Chemistry, 2007, 606, 150-158.	3.8	9
358	SnO2–poly(diallyldimethylammonium chloride) films: Electrochemical evidence for heme protein absorption, denaturation, and demetallation. Journal of Electroanalytical Chemistry, 2007, 610, 28-36.	3.8	10
359	Layer-by-layer deposition of open-pore mesoporous TiO2-Nafion® film electrodes. Journal of Solid State Electrochemistry, 2007, 11, 1109-1117.	2.5	16
360	Layer-by-layer deposition of praseodymium oxide on tin-doped indium oxide (ITO) surface. Sensors and Actuators B: Chemical, 2007, 123, 400-406.	7.8	7

#	Article	IF	CITATIONS
361	Capillary electrophoresis with microwave-enhanced electrochemical detection. Analyst, The, 2006, 131, 1210.	3.5	13
362	The electrochemical ion-transfer reactivity of porphyrinato metal complexes in 4-(3-phenylpropyl)pyridine water systems. New Journal of Chemistry, 2006, 30, 327.	2.8	23
363	Electrochemical properties of core-shell TiC–TiO2nanoparticle films immobilized at ITO electrode surfaces. Physical Chemistry Chemical Physics, 2006, 8, 5437-5443.	2.8	33
364	Electrochemical Deposition of Praseodymium Oxide on Tin-Doped Indium Oxide as a Thin Sensing Film. Journal of the Electrochemical Society, 2006, 153, C517.	2.9	17
365	Microwave Induced Jet Boiling Investigated via Voltammetry at Ringâ disk Microelectrodes. Journal of Physical Chemistry B, 2006, 110, 17589-17594.	2.6	25
366	Self-Supported Methoxylation and Acetoxylation Electrosynthesis Using a Simple Thin-Layer Flow Cell. Journal of the Electrochemical Society, 2006, 153, D143.	2.9	56
367	New bis(triazinyl) pyridines for selective extraction of americium(iii). New Journal of Chemistry, 2006, 30, 1171.	2.8	162
368	Comparison of three optimized digestion methods for rapid determination of chemical oxygen demand: Closed microwaves, open microwaves and ultrasound irradiation. Analytica Chimica Acta, 2006, 561, 210-217.	5.4	57
369	Focused microwaves in electrochemical processes. Electrochimica Acta, 2006, 51, 2195-2203.	5.2	37
370	Synthesis, structure, and redox states of homoleptic d-block metal complexes with bis-1,2,4-triazin-3-yl-pyridine and 1,2,4-triazin-3-yl-bipyridine extractants. Polyhedron, 2006, 25, 888-900.	2.2	47
371	lon transfer processes at the room temperature ionic liquid aqueous solution interface supported by a hydrophobic carbon nanofibers – silica composite film. Journal of Electroanalytical Chemistry, 2006, 587, 133-139.	3.8	37
372	Towards paired and coupled electrode reactions for clean organic microreactor electrosyntheses. Journal of Applied Electrochemistry, 2006, 36, 617-634.	2.9	161
373	A rotating disc voltammetry study of the 1,8-dihydroxyanthraquinone mediated reduction of colloidal indigo. Journal of Solid State Electrochemistry, 2006, 10, 865-871.	2.5	23
374	Characterisation of hydrophobic carbon nanofiber–silica composite film electrodes for redox liquid immobilisation. Electrochimica Acta, 2006, 51, 5897-5903.	5.2	29
375	Self-Supported and Clean One-Step Cathodic Coupling of Activated Olefins with Benzyl Bromide Derivatives in a Micro Flow Reactor. Angewandte Chemie - International Edition, 2006, 45, 4146-4149.	13.8	100
376	Storing and Releasing Hydrogen with a Redox Switch. Angewandte Chemie - International Edition, 2006, 45, 6005-6008.	13.8	20
377	Microwave Activation of Processes in Mesopores: The Thiourea Electrooxidation at Mesoporous Platinum. Electroanalysis, 2006, 18, 793-800.	2.9	14
378	Characterisation of biphasic electrodes based on the liquid N,N-didodecyl-N′N′-diethylphenylenediamine redox system immobilised on porous hydrophobic silicates and immersed in aqueous media. Journal of Electroanalytical Chemistry, 2005, 582, 202-208.	3.8	11

#	Article	IF	CITATIONS
379	Assembly of thin mesoporous titania films and their effects on the voltammetry of weakly adsorbing redox systems. Journal of Electroanalytical Chemistry, 2005, 579, 267-275.	3.8	14
380	Electrolyte free electro-organic synthesis: The cathodic dimerisation of 4-nitrobenzylbromide in a micro-gap flow cell. Electrochemistry Communications, 2005, 7, 918-924.	4.7	55
381	A novel cation-binding TiO2 nanotube substrate for electro- and bioelectro-catalysis. Electrochemistry Communications, 2005, 7, 1050-1058.	4.7	89
382	Mesoporous platinum hosts for electrodeâ^£liquidâ^£liquid – Triple phase boundary redox systems. Electrochemistry Communications, 2005, 7, 1333-1339.	4.7	35
383	Self-supported paired electrosynthesis of 2,5-dimethoxy-2,5-dihydrofuran using a thin layer flow cell without intentionally added supporting electrolyte. Electrochemistry Communications, 2005, 7, 35-39.	4.7	97
384	Microphase voltammetry of diluted and undiluted redox liquids deposited on sol–gel ceramic carbon electrodes. Electrochimica Acta, 2005, 50, 1711-1717.	5.2	16
385	Liquid–liquid interfacial processes at hydrophobic silica carbon composite electrodes: ion transfer at water–nitrobenzene, water–o-nitrophenyloctylether, and at water–o-nitrophenylphenylether interfaces. Electrochimica Acta, 2005, 50, 2315-2322.	5.2	28
386	Microwave Activation of Electrochemical Processes at Glassy Carbon and Boron-Doped Diamond Electrodes. Electroanalysis, 2005, 17, 385-391.	2.9	17
387	TiO2 phytate films as hosts and conduits for cytochrome c electrochemistry. Bioelectrochemistry, 2005, 66, 41-47.	4.6	34
388	Effects of carbon nanofiber composites on electrode processes involving liquid liquid ion transfer. Journal of Solid State Electrochemistry, 2005, 9, 874-881.	2.5	18
389	Microwave-enhanced electrochemical processes in micellar surfactant media. Journal of Solid State Electrochemistry, 2005, 9, 809-815.	2.5	17
390	Simple Cast-Deposited Multi-Walled Carbon Nanotube/Nafionâ"¢ Thin Film Electrodes for Electrochemical Stripping Analysis. Mikrochimica Acta, 2005, 150, 269-276.	5.0	37
391	Cyclic Voltammetry. , 2005, , 51-97.		3
392	Ion transfer processes at 4-(3-phenylpropyl)-pyridine aqueous electrolyte electrode triple phase boundary systems supported by graphite and by mesoporous TiO2. Faraday Discussions, 2005, 129, 219.	3.2	32
393	Microwave enhanced electroanalysis of formulations: processes in micellar media at glassy carbon and at platinum electrodes. Analyst, The, 2005, 130, 1425.	3.5	17
394	Mesoporous TiO2carboxymethyl- \hat{I}^3 -cyclodextrate multi-layer host films: effects on adsorption and electrochemistry of 1,1 $\hat{a}\in^2$ -ferrocenedimethanol. Analyst, The, 2005, 130, 358-363.	3.5	13
395	Redox Processes in Mesoporous Oxide Membranes:Â Layered TiO2Phytate and TiO2Flavin Adenine Dinucleotide Films. Langmuir, 2005, 21, 9482-9487.	3.5	37
396	Microwave activation of the electro-oxidation of glucose in alkaline media. Physical Chemistry Chemical Physics, 2005, 7, 3552.	2.8	32

#	Article	IF	CITATIONS
397	UV/Vis/NIR Spectroelectrochemistry. , 2005, , 167-189.		О
398	Electrifying interfaces. Philosophical Transactions Series A, Mathematical, Physical, and Engineering Sciences, 2004, 362, 2611-2633.	3.4	4
399	Electrochemical Detection of As(III) via Iodine Electrogenerated at Platinum, Gold, Diamond or Carbon-Based Electrodes. Electroanalysis, 2004, 16, 897-903.	2.9	40
400	Electrochemistry in the Presence of Mesoporous TiO2 Phytate Nanofilms. Electroanalysis, 2004, 16, 89-96.	2.9	21
401	Electrochemical reactivity of TiO2 nanoparticles adsorbed onto boron-doped diamond surfaces. Electrochemistry Communications, 2004, 6, 1153-1158.	4.7	42
402	Microwave enhanced electrochemistry: mass transport effects and steady state voltammetry in the sub-millisecond time domain. Journal of Electroanalytical Chemistry, 2004, 573, 175-182.	3.8	37
403	Electroanalytical thin film electrodes based on a Nafion? ? multi-walled carbon nanotube composite. Electrochemistry Communications, 2004, 6, 917-922.	4.7	60
404	Hemoglobin adsorption into TiO2 phytate multi-layer films: particle size and conductivity effects. Electrochemistry Communications, 2004, 6, 1249-1253.	4.7	49
405	Microwave activation in ionic liquids induces high temperature–high speed electrochemical processes. Chemical Communications, 2004, , 2816-2817.	4.1	7
406	Hydrophobic silica sol–gel films for biphasic electrodes and porotrodes. Analyst, The, 2004, 129, 1181-1185.	3.5	14
407	Microwave effects on the electrochemical deposition of copper. New Journal of Chemistry, 2004, 28, 1544.	2.8	24
408	Large-Amplitude Fourier Transformed High-Harmonic Alternating Current Cyclic Voltammetry:Â Kinetic Discrimination of Interfering Faradaic Processes at Glassy Carbon and at Boron-Doped Diamond Electrodes. Analytical Chemistry, 2004, 76, 3619-3629.	6.5	67
409	Liquid Liquid Ion-Transfer Processes at the Dioctylphosphoric Acid (N,N-didodecyl-Nâ€~,Nâ€~-diethylphenylenediamine) Water (Electrolyte) Interface at Graphite and Mesoporous TiO2Substrates. Analytical Chemistry, 2004, 76, 5364-5369.	6.5	15
410	Electrochemically driven reversible solid state metal exchange processes in polynuclear copper complexes. Journal of Solid State Electrochemistry, 2003, 7, 141-146.	2.5	14
411	Electroanalysis at Diamond-Like and Doped-Diamond Electrodes. Electroanalysis, 2003, 15, 1349-1363.	2.9	331
412	Nanodiamond Thin Film Electrodes: Metal Electro-Deposition and Stripping Processes. Electroanalysis, 2003, 15, 169-174.	2.9	13
413	Electrodeposition of Lead at Boron-Doped Diamond Film Electrodes: Effect of Temperature. Electroanalysis, 2003, 15, 1011-1016.	2.9	14
414	Sonoelectrochemistry of molecular and colloidal redox systems at carbon nanofiber–ceramic composite electrodes. Electrochimica Acta, 2003, 48, 3411-3417.	5.2	19

#	Article	IF	CITATIONS
415	Adsorption and redox processes at carbon nanofiber electrodes grown onto a ceramic fiber backbone. Electrochemistry Communications, 2003, 5, 51-55.	4.7	28
416	Quartz crystal microbalance monitoring of density changes in mesoporous TiO2 phytate films during redox and ion exchange processes. Electrochemistry Communications, 2003, 5, 286-291.	4.7	5
417	Electrochemical and related processes at surface conductive diamond–solution interfaces. Physica Status Solidi A, 2003, 199, 49-55.	1.7	3
418	Accumulation and Reactivity of the Redox Protein Cytochromecin Mesoporous Films of TiO2Phytate. Langmuir, 2003, 19, 4327-4331.	3.5	116
419	Influence of thin film properties on the electrochemical performance of diamond electrodes. Diamond and Related Materials, 2003, 12, 590-595.	3.9	30
420	Anodic activity of boron-doped diamond electrodes in bleaching processes: effects of ultrasound and surface states. New Journal of Chemistry, 2003, 27, 698-703.	2.8	23
421	Electrochemistry of immobilised redox droplets: Concepts and applications. Physical Chemistry Chemical Physics, 2003, 5, 4053.	2.8	179
422	Nanodiamond Thin Films on Titanium Substrates. Journal of the Electrochemical Society, 2003, 150, E59.	2.9	30
423	Electrochemical Characterization of Hydrous Ruthenium Oxide Nanoparticle Decorated Boron-Doped Diamond Electrodes. Electrochemical and Solid-State Letters, 2002, 5, E47.	2.2	25
424	Microwave Activation of Electrochemical Processes:Â Enhanced Electrodehalogenation in Organic Solvent Media. Journal of the American Chemical Society, 2002, 124, 9784-9788.	13.7	67
425	Electrochemical Analysis of Solids. A Review. Collection of Czechoslovak Chemical Communications, 2002, 67, 163-208.	1.0	200
426	Probing Thermodynamic Aspects of Electrochemically Driven Ion-Transfer Processes Across Liquid Liquid Interfaces:  Pure versus Diluted Redox Liquids. Journal of Physical Chemistry B, 2002, 106, 8697-8704.	2.6	57
427	Nanoporous iron oxide membranes: layer-by-layer deposition and electrochemical characterisation of processes within nanopores. New Journal of Chemistry, 2002, 26, 625-629.	2.8	50
428	An Electrochemical Redox Couple Activitated by Microelectrodes for Confined Chemical Patterning of Surfaces. Analytical Chemistry, 2002, 74, 1590-1596.	6.5	34
429	The direct electrochemistry of ferritin compared with the direct electrochemistry of nanoparticulate hydrous ferric oxide. New Journal of Chemistry, 2002, 26, 259-263.	2.8	49
430	Electrochemical analysis of nucleic acids at boron-doped diamond electrodes. Analyst, The, 2002, 127, 329-332.	3.5	82
431	Voltammetric analysis of iron oxide pigments. Analyst, The, 2002, 127, 1100-1107.	3.5	47
432	Abrasive stripping voltammetry of silver and tin at boron-doped diamond electrodes. Diamond and Related Materials, 2002, 11, 646-650.	3.9	27

#	Article	IF	CITATIONS
433	Chromate and Dichromate Electro-Insertion Processes into a N,N,N′,N′-Tetraoctylphenylenediamine Redox Liquid. Electroanalysis, 2002, 14, 172.	2.9	25
434	Simultaneous Electrochemical Detection and Determination of Lead and Copper at Boron-Doped Diamond Film Electrodes. Electroanalysis, 2002, 14, 262-272.	2.9	93
435	Reduction of Tetrachloroaurate(III) at Boron-Doped Diamond Electrodes: Gold Deposition Versus Gold Colloid Formation. Electroanalysis, 2002, 14, 797.	2.9	30
436	Detection of Chlorophenols in Aqueous Solution via Hydrodynamic Channel Flow Cell Voltammetry Using a Boron-Doped Diamond Electrode. Electroanalysis, 2002, 14, 975.	2.9	26
437	Deposition and characterisation of a porous Sn(IV) semiconductor nanofilm on boron-doped diamond. Journal of Solid State Electrochemistry, 2002, 6, 183-187.	2.5	13
438	Direct cytochrome c electrochemistry at boron-doped diamond electrodes. Electrochemistry Communications, 2002, 4, 62-66.	4.7	77
439	Phosphate and arsenate electro-insertion processes into a N,N,N′,N′-tetraoctylphenylenediamine redox liquid. Electrochemistry Communications, 2002, 4, 462-467.	4.7	49
440	Paired electrosynthesis: micro-flow cell processes with and without added electrolyte. Electrochemistry Communications, 2002, 4, 825-831.	4.7	93
441	Adsorption and reactivity of hydrous iron oxide nanoparticles on boron-doped diamond. Electrochemistry Communications, 2002, 4, 820-824.	4.7	17
442	Directed assembly of multilayers—the case of Prussian Blue. Chemical Communications, 2001, , 1994-1995.	4.1	74
443	Sono-emulsion electrosynthesis: electrode-insensitive Kolbe reactions. Chemical Communications, 2001, , 87-88.	4.1	27
444	Mechanistic aspects of the sonoelectrochemical degradation of the reactive dye Procion Blue at boron-doped diamond electrodes. Diamond and Related Materials, 2001, 10, 662-666.	3.9	33
445	Nanocomposite electrodes made of carbon nanofibers and black wax. Anodic stripping voltammetry of zinc and lead. Analyst, The, 2001, 126, 1878-1881.	3.5	22
446	Enhanced chemical reversibility of redox processes in cyanine dye rotaxanes. Chemical Communications, 2001, , 1046-1047.	4.1	53
447	Electrochemically Driven Ion Insertion Processes across Liquid Liquid Boundaries:  Neutral versus Ionic Redox Liquids. Journal of Physical Chemistry B, 2001, 105, 1344-1350.	2.6	68
448	Direct electrochemistry of nanoparticulate Fe2O3 in aqueous solution and adsorbed onto tin-doped indium oxide. Pure and Applied Chemistry, 2001, 73, 1885-1894.	1.9	63
449	Biphasic sonoelectrosynthesis. A review. Pure and Applied Chemistry, 2001, 73, 1947-1955.	1.9	48
450	Fast electrochemical triple-interface processes at boron-doped diamond electrodes. Journal of Solid State Electrochemistry, 2001, 5, 88-93.	2.5	24

#	Article	IF	CITATIONS
451	Microwave activation of electrochemical processes: enhanced PbO2 electrodeposition, stripping and electrocatalysis. Journal of Solid State Electrochemistry, 2001, 5, 313-318.	2.5	24
452	Photoelectrochemically driven processes at the N,N,N′,N′-tetrahexylphenylenediamine microdroplet electrode aqueous electrolyte triple interface. Journal of Solid State Electrochemistry, 2001, 5, 301-305.	2.5	30
453	Voltammetry of electroactive liquid redox systems: anion insertion and chemical reactions in microdroplets of para -tetrakis(6-methoxyhexyl) phenylenediamine, para - and meta -tetrahexylphenylenediamine. Journal of Solid State Electrochemistry, 2001, 5, 17-22.	2.5	31
454	Voltammetry at carbon nanofiber electrodes. Electrochemistry Communications, 2001, 3, 177-180.	4.7	66
455	Microwave Activation of Electrochemical Processes: Square-Wave Voltammetric Stripping Detection of Cadmiumin the Presence of the Surfactant Triton X. Electroanalysis, 2001, 13, 639-645.	2.9	36
456	Microwave-Enhanced Anodic Stripping Detection of Lead in a River Sediment Sample. A Mercury-Free Procedure Employing a Boron-Doped Diamond Electrode. Electroanalysis, 2001, 13, 831-835.	2.9	60
457	Low-temperature sonoelectrochemical processes. Journal of Electroanalytical Chemistry, 2001, 507, 144-151.	3.8	16
458	Emulsion electrosynthesis in the presence of power ultrasound Biphasic Kolbe coupling processes at platinum and boron-doped diamond electrodes. Journal of Electroanalytical Chemistry, 2001, 507, 135-143.	3.8	56
459	Low-temperature sonoelectrochemical processes. Journal of Electroanalytical Chemistry, 2001, 506, 170-177.	3.8	22
460	Sonoelectrochemistry at platinum and boron-doped diamond electrodes: achieving â€~fast mass transport' for â€~slow diffusers'. Journal of Electroanalytical Chemistry, 2001, 513, 94-99.	3.8	30
461	Stability of Mercury Film Electrodes under the Influence of High Frequency (500kHz) Ultrasound. Journal of Applied Electrochemistry, 2001, 31, 475-480.	2.9	8
462	Lead Dioxide Deposition and Electrocatalysis at Highly Boron-Doped Diamond Electrodes in the Presence of Ultrasound. Journal of the Electrochemical Society, 2001, 148, E66.	2.9	36
463	Surface Modification of Chemical Vapor Deposited Diamond Induced by Power Ultrasound:â€,An X-Ray Photoelectron Spectroscopy Study. Electrochemical and Solid-State Letters, 2001, 4, E29.	2.2	11
464	Microwave Activated Voltammetry: The Thermally Enhanced Anodic Stripping Detection of Cadmium. Electroanalysis, 2000, 12, 267-273.	2.9	40
465	Voltammetry of Electroactive Oil Droplets. Part I: Numerical Modelling for Three Mechanistic Models Using the Dual Reciprocity Finite Element Method. Electroanalysis, 2000, 12, 1012-1016.	2.9	29
466	Voltammetry of Electroactive Oil Droplets. Part II: Comparison of Experimental and Simulation Data for Coupled Ion and Electron Insertion Processes and Evidence for Microscale Convection. Electroanalysis, 2000, 12, 1017-1025.	2.9	60
467	Photochemical and electrochemical behavior of thiophene-S-oxides. Journal of Physical Organic Chemistry, 2000, 13, 648-653.	1.9	30
468	Thermal activation of electrochemical processes in a Rf-heated channel flow cell: experiment and finite element simulation. Journal of Electroanalytical Chemistry, 2000, 492, 150-155.	3.8	46

#	Article	IF	CITATIONS
469	lonic liquid modified electrodes. Unusual partitioning and diffusion effects of Fe(CN)64â^'/3â^' in droplet and thin layer deposits of 1-methyl-3-(2,6-(S)-dimethylocten-2-yl)-imidazolium tetrafluoroborate. Journal of Electroanalytical Chemistry, 2000, 493, 75-83.	3.8	126
470	Electrochemical detection of sulphide: a novel dual flow cell. Sensors and Actuators B: Chemical, 2000, 69, 189-192.	7.8	31
471	Sonoelectrochemical and sonochemical effects of cavitation: correlation with interfacial cavitation induced by 20 kHz ultrasound. Ultrasonics Sonochemistry, 2000, 7, 7-14.	8.2	65
472	Sonoelectrochemistry at highly boron-doped diamond electrodes: silver oxide deposition and electrocatalysis in the presence of ultrasound. Journal of Solid State Electrochemistry, 2000, 4, 383-389.	2.5	17
473	Sonoelectrochemical investigation of silver analysis at a highly boron-doped diamond electrode. Talanta, 2000, 53, 403-415.	5.5	43
474	Microwave activation of electrochemical processes: convection, thermal gradients and hot spot formation at the electrodeâ^£solution interface. New Journal of Chemistry, 2000, 24, 653-658.	2.8	52
475	Clostridium isatidis colonised carbon electrodes: voltammetric evidence for direct solid state redox processes. New Journal of Chemistry, 2000, 24, 179-181.	2.8	38
476	Modeling Hot Wire Electrochemistry. Coupled Heat and Mass Transport at a Directly and Continuously Heated Wire. Journal of Physical Chemistry B, 2000, 104, 764-769.	2.6	45
477	Unusually Fast Electron and Anion Transport Processes Observed in the Oxidation of "Electrochemically Open―Microcrystalline [{M(bipy)2}{Mâ€~(bipy)2}(μ-L)](PF6)2Complexes (M, Mâ€~ = I Solidâ^'Electrodeâ^'Aqueous Electrolyte Interface. Iournal of Physical Chemistry B. 2000. 104. 1977-1983.	Ru, Oş;) Tj 2.6	ETQg1 1 0.7
478	Laser Activation Voltammetry:Â Selective Removal of Reduced Forms of Methyl Viologen Deposited on Glassy Carbon and Boron-Doped Diamond Electrodes. Analytical Chemistry, 2000, 72, 2362-2370.	6.5	37
479	Electrochemically induced surface modifications of boron-doped diamond electrodes: an X-ray photoelectron spectroscopy study. Diamond and Related Materials, 2000, 9, 390-396.	3.9	154
480	Water-induced accelerated ion diffusion: voltammetric studies in 1-methyl-3-[2,6-(S)-dimethylocten-2-yl]imidazolium tetrafluoroborate, 1-butyl-3-methylimidazolium tetrafluoroborate and hexafluorophosphate ionic liquids. New Journal of Chemistry, 2000, 24, 1009-1015.	2.8	513
481	Voltammetry at Boron-Doped Diamond Electrodes in Liquid Ammonia: Solvent Window Effects and Diamond Surface Modification. Electrochemical and Solid-State Letters, 1999, 3, 224.	2.2	16
482	Low-temperature sonoelectrochemical processes. Journal of Electroanalytical Chemistry, 1999, 477, 71-78.	3.8	30
483	High-frequency sonoelectrochemical processes: mass transport, thermal and surface effects induced by cavitation in a 500 kHz reactor. Ultrasonics Sonochemistry, 1999, 6, 189-197.	8.2	39
484	Novel features associated with the electrochemically driven bis(η5-pentaphenylcyclopentadienyl)iron(II)–iron(III) redox transformation at an electrode–microcrystal–solvent (electrolyte) interface. Inorganica Chimica Acta, 1999, 291, 21-31.	2.4	11
485	Methylene Green Voltammetry in Aqueous Solution:  Studies Using Thermal, Microwave, Laser, or Ultrasonic Activation at Platinum Electrodes. Journal of Physical Chemistry B, 1999, 103, 9987-9995.	2.6	46
486	Sono-Cathodic Stripping Voltammetry of Lead at a Polished Boron-Doped Diamond Electrode: Application to the Determination of Lead in River Sediment. Electroanalysis, 1999, 11, 1083-1088.	2.9	79

#	Article	IF	CITATIONS
487	Complex Electron Transfer Kinetic Data from Convolution Analysis of Cyclic Voltammograms. Theory and Application to Diamond Electrodes. Electroanalysis, 1999, 11, 1149-1154.	2.9	16
488	Sonoelectrochemistry at tungsten-supported boron-doped CVD diamond electrodes. Diamond and Related Materials, 1999, 8, 824-829.	3.9	34
489	Electron induced modification of the surface electrochemical properties of diamond electrodes. Chemical Communications, 1999, , 1697-1698.	4.1	7
490	The 20 kHz sonochemical degradation of trace cyanide and dye stuffs in aqueous media. New Journal of Chemistry, 1999, 23, 845-849.	2.8	41
491	Sulfide accumulation and sensing based on electrochemical processes in microdroplets of N1-[4-(dihexylamino)phenyl]-N1,N4,N4-trihexyl-1,4-phenylenediamine. Chemical Communications, 1999, , 1823-1824.	4.1	21
492	Evidence for Nucleation-Growth, Redistribution, and Dissolution Mechanisms during the Course of Redox Cycling Experiments on the C60/NBu4C60Solid-State Redox System:Â Voltammetric, SEM, and in Situ AFM Studies. Journal of Physical Chemistry B, 1999, 103, 5637-5644.	2.6	62
493	Complex Electron Transfer Kinetic Data from Convolution Analysis of Cyclic Voltammograms. Theory and Application to Diamond Electrodes. Electroanalysis, 1999, 11, 1149-1154.	2.9	Ο
494	Sonoelectrochemically modified electrodes: ultrasound assisted electrode cleaning, conditioning, and product trapping in 1-octanol/water emulsion systems. Electrochimica Acta, 1998, 43, 2157-2165.	5.2	46
495	Sono-electroanalysis: Application to the detection of lead in wine. Electrochimica Acta, 1998, 43, 3443-3449.	5.2	57
496	The Use of Sonotrodes for Electroanalysis:Sono-ASV Detection of Lead in Aqueous Solution. Electroanalysis, 1998, 10, 26-32.	2.9	30
497	Sonoelectrochemistry in Highly Resistive Media:Mass Transport Effects. Electroanalysis, 1998, 10, 562-566.	2.9	12
498	Anion Detection by Electro-Insertion intoN,N,N′, N′-Tetrahexyl-Phenylenediamine (THPD) Microdroplets Studied by Voltammetry, EQCM, and SEM Techniques. Electroanalysis, 1998, 10, 821-826.	2.9	66
499	Sonoelectrochemically Enhanced Electrocatalytic Processes: The Pb(IV) Catalyzed Cleavage of 1,2-cis-Cyclopentanediol at Graphite and Glassy Carbon Electrodes. Electroanalysis, 1998, 10, 1188-1192.	2.9	15
500	Electrochemistry at boron-doped diamond films grown on graphite substrates: redox-, adsorption and deposition processes. Journal of Electroanalytical Chemistry, 1998, 442, 207-216.	3.8	69
501	lon pair formation between the electrogenerated 2,3-dichloro-5,6-dicyano-1,4-benzoquinone dianion and the sodium ion at platinum surfaces. Journal of Electroanalytical Chemistry, 1998, 451, 193-201.	3.8	21
502	Mechanistic Aspects of the Electrochemical Reduction of 7,7,8,8-Tetracyanoquinodimethane in the Presence of Mg2+or Ba2+. Journal of Physical Chemistry B, 1998, 102, 6588-6595.	2.6	28
503	Microwave activation of electrochemical processes at microelectrodes. Chemical Communications, 1998, , 2595-2596.	4.1	63
504	Sonoelectrochemical production of hydrogen peroxide at polished boron-doped diamond electrodes. Chemical Communications, 1998, , 1961-1962.	4.1	22

#	Article	IF	CITATIONS
505	High-Pressure Sonoelectrochemistry in Aqueous Solution: Soft Cavitation under CO2. Journal of Physical Chemistry A, 1998, 102, 8888-8893.	2.5	22
506	Mechanistic Aspects of the Electrocatalytic Oxidative Cleavage of 1,2-Diols by Electrogenerated Pb(IV). Journal of Physical Chemistry B, 1998, 102, 1186-1192.	2.6	10
507	EPR Studies Associated with the Electrochemical Reduction of C60 and Supramolecular Complexes of C60 in Tolueneâ ^{~,} Acetonitrile Solvent Mixtures. Journal of Physical Chemistry A, 1998, 102, 2641-2649.	2.5	27
508	The Use of Sonotrodes for Electroanalysis:Sono-ASV Detection of Lead in Aqueous Solution. Electroanalysis, 1998, 10, 26-32.	2.9	0
509	Sonoelectrochemistry in Highly Resistive Media:Mass Transport Effects. Electroanalysis, 1998, 10, 562-566.	2.9	Ο
510	Sonovoltammetry of Oxygen at Cuâ€Ni Alloy Electrodes: Activation of Alloy Electrodes and Sonoâ€Ringâ€Disk Voltammetry. Journal of the Electrochemical Society, 1997, 144, 3019-3026.	2.9	20
511	The electrochemical reduction of indigo dissolved in organic solvents and as a solid mechanically attached to a basal plane pyrolytic graphite electrode immersed in aqueous electrolyte solution. Journal of the Chemical Society Perkin Transactions II, 1997, , 1735-1742.	0.9	112
512	Coupled Redox Reactions, Linkage Isomerization, Hydride Formation, and Acidâ^'Base Relationships in the Decaphenylferrocene System. Organometallics, 1997, 16, 2787-2797.	2.3	17
513	Voltammetric, Specular Reflectance Infrared, and X-ray Electron Probe Characterization of Redox and Isomerization Processes Associated with the [Mn(CO)2(η3-P2Pâ€~)Br]+/0 (P2Pâ€~ = {Ph2P(CH2)2}2PPh), [Mn(CO)2(η3-P3Pâ€~)Br]+/0 (P3Pâ€~ = {Ph2PCH2}3P), and [{Mn(CO)2(η2-dpe)Br}2(μ-dpe)]2+/0 (dpe =) Tj ET	Qq1·1 0.7	84314 rgBT /(
514	Ultrasound-assisted electrochemical reduction of emulsions in aqueous media. Chemical Communications, 1997, , 995-996.	4.1	16
515	Electrolysis in the presence of ultrasound: cell geometries for the application of extreme rates of mass transfer in electrosynthesis. Journal of the Chemical Society Perkin Transactions II, 1997, , 2055-2059.	0.9	19
516	Homogeneous and heterogeneous catalytic redox processes: solution and solid state voltammetry of lead complexes at carbon electrodes. Journal of Electroanalytical Chemistry, 1997, 424, 25-34.	3.8	18
517	A novel approach for the quantitative kinetic study of reactions at solid/liquid interfaces in the presence of power ultrasound. Ultrasonics Sonochemistry, 1997, 4, 1-7.	8.2	13
518	Ultrasound in photoelectrochemistry: A new approach to the enhancement of the efficiency of semiconductor electrode processes. Ultrasonics Sonochemistry, 1997, 4, 223-228.	8.2	15
519	Redox processes in microdroplets studied by voltammetry, microscopy and ESR spectroscopy: oxidation ofN,N,N′,N′-tetrahexylphenylene diamine deposited on solid electrode surfaces and immersed in aqueous electrolyte solution. Journal of Electroanalytical Chemistry, 1997, 437, 209-218.	3.8	174
520	The use of ultrasound in the enhancement of the deposition and detection of metals in anodic stripping voltammetry. Electroanalysis, 1997, 9, 19-22.	2.9	53
521	Applications of the channel flow cell for UV-visible spectroelectrochemical studies. Part 2: Transient signals. Electroanalysis, 1997, 9, 284-287.	2.9	18
522	Sonoelectrochemical processes: A review. Electroanalysis, 1997, 9, 509-522.	2.9	262

#	Article	IF	CITATIONS
523	Dual activation: coupling ultrasound to electrochemistry—an overview. Electrochimica Acta, 1997, 42, 2919-2927.	5.2	145
524	Electrochemical and X-ray diffraction study of the redox cycling of nanocrystals of 7,7,8,8-tetracyanoquinodimethane. Observation of a solid–solid phase transformation controlled by nucleation and growth. Journal of the Chemical Society, Faraday Transactions, 1996, 92, 3925-3933.	1.7	108
525	Voltammetry in the Presence of Ultrasound:Â Sonovoltammetric Detection of Cytochromecunder Very Fast Mass Transport Conditions. The Journal of Physical Chemistry, 1996, 100, 17395-17399.	2.9	40
526	Sonovoltammetric measurement of the rates of electrode processes with fast coupled homogeneous kinetics: making macroelectrodes behave like microelectrodes. Chemical Communications, 1996, , 1017.	4.1	32
527	Voltammetric monitoring of photochemical reactions: Photo-induced electron transfer top-chloronitrobenzene. Electroanalysis, 1996, 8, 515-518.	2.9	3
528	Detection of new features associated with the oxidation of microcrystalline tetrathiafulvalene attached to gold electrodes by the simultaneous application of electrochemical and quartz crystal microbalance techniques. Electroanalysis, 1996, 8, 732-741.	2.9	46
529	Electrode processes at the surfaces of sonotrodes. Electrochimica Acta, 1996, 41, 315-320.	5.2	41
530	Voltammetry in the presence of ultrasound: A novel sono-electrode geometry. Electrochimica Acta, 1996, 41, 1541-1547.	5.2	42
531	Electrochemistry in the presence of ultrasound: the need for bipotentiostatic control in sonovoltammetric experiments. Ultrasonics Sonochemistry, 1996, 3, S131-S134.	8.2	46
532	Simultaneous electrochemical and quartz crystal microbalance studies of non-conducting microcrystalline particles of trans-Cr(CO)2(dpe)2 and trans-[Cr(CO)2(dpe)2]+ (dpe = Ph2PCH2CH2PPh2) attached to gold electrodes. Journal of Electroanalytical Chemistry, 1996, 404, 227-235.	3.8	34
533	Voltammetry in the presence of ultrasound: surface and solution processes in the sonovoltammetric reduction of nitrobenzene at glassy carbon and gold electrodes. Journal of Electroanalytical Chemistry, 1996, 414, 95-105.	3.8	13
534	Voltammetry in the presence of ultrasound: the limit of acoustic streaming induced diffusion layer thinning and the effect of solvent viscosity. Journal of Electroanalytical Chemistry, 1996, 415, 55-63.	3.8	114
535	Voltammetry in the presence of ultrasound: surface and solution processes in the sonovoltammetric reduction of nitrobenzene at glassy carbon and gold electrodes1. Journal of Electroanalytical Chemistry, 1996, 414, 95-105.	3.8	33
536	Characterization of titanocene(III) complexes of β-diketonates by electrochemical, spectroscopic and crystallographic methods: stabilization of oxidized and reduced β-diketonate radicals by acetyl and titanocene derivatization, respectively. Inorganica Chimica Acta, 1995, 235, 117-126.	2.4	13
537	Redox and electroinsertion processes associated with the voltammetry of microcrystalline forms of Dawson molybdate anion salts mechanically attached to graphite electrodes and immersed in aqueous electrolyte media. Journal of Electroanalytical Chemistry, 1995, 396, 407-418.	3.8	54
538	Voltammetry in the presence of ultrasound: Can ultrasound modify heterogeneous electron transfer kinetics?. Journal of Electroanalytical Chemistry, 1995, 395, 335-339.	3.8	106
539	Electrochemical Oxidation and Reduction of Cationic Carbonyl Hydride Complexes of Group VI Transition Metals. Inorganic Chemistry, 1995, 34, 1705-1710.	4.0	29
540	Electrochemical Study of Microcrystalline Solid Prussian Blue Particles Mechanically Attached to Graphite and Gold Electrodes: Electrochemically Induced Lattice Reconstruction. The Journal of Physical Chemistry, 1995, 99, 2096-2103.	2.9	164

#	Article	IF	CITATIONS
541	Oraganic sonoelectrochemistry. Reduction of fluorescein in the presence of 20 kHz power ultrasound: an EC? reaction. Journal of the Chemical Society Perkin Transactions II, 1995, , 1981.	0.9	15
542	Mechanistic Study of the Voltammetry of Nonconducting Microcrystalline cis- and trans-Cr(CO)2(dpe)2 Complexes (dpe = Ph2PCH2CH2PPh2) Mechanically attached to a Graphite Electrode and Immersed in Different Aqueous Electrolyte Media: Identification by Infrared Spectroscopy of cis-[Cr(CO)2(dpe)2]+ Stabilized at the Electrode-Solid-Solution Interface. Organometallics, 1994, 13, 5122-5131.	2.3	41
543	Crystal structure of twinned (η5-C5(CH3)4CF3) (η5-C5(CH3)5)Ru. Structural Chemistry, 1994, 5, 177-181.	2.0	5
544	Mechanistic aspects of the electron and ion transport processes across the electrode solid solvent (electrolyte) interface of microcrystalline decamethylferrocene attached mechanically to a graphite electrode. Journal of Electroanalytical Chemistry, 1994, 372, 125-135.	3.8	97
545	Triple-decker complexes. 9. Triple-decker complexes with bridging cyclopentadienyl ligands and novel cyclopentadienyl transfer reactions. Organometallics, 1993, 12, 4039-4045.	2.3	75
546	Voltammetry, electron microscopy, and x-ray electron probe microanalysis at the electrode-aqueous electrolyte interface of solid microcrystalline cis- and trans-Cr(CO)2(dpe)2 and trans-[Cr(CO)2(dpe)2]+ complexes (dpe = Ph2PCH2CH2PPh2) mechanically attached to carbon electrodes. Journal of the American Chemical Society, 1993, 115, 9556-9562.	13.7	70
547	Novel sandwich cations of platinum with tetramethyl-cyclobutadiene and cyclopentdienyl or hexamethylbenzene ligands. Journal of the Chemical Society Dalton Transactions, 1993, , 1979.	1.1	20
548	Di- and tri-metal compounds prepared from the alkylidyne molybdenum complexes [Mo(î—¼CR)(CO)2(ÎC5H5)] (R = C6H4OMe-2, C6H4NMe2-4 or C6H3Me2-2,6) and [MoFe(μ-CC6H4Me-4)(CO)6(ÎC5H5)]. Journal of Organometallic Chemistry, 1989, 363, 311-323.	1.8	12
549	Chemistry of polynuclear metal complexes with bridging carbene or carbyne ligands. Part 79. Synthesis and reactions of the alkylidynemetal complexes [M(CR)(CO)2(Î+C5H5)](R = C6H3Me2-2,6, M = Cr,) T [MoFe(µ-CC6H3Me2-2,6)(CO)5(Î+C5H5)]. Journal of the Chemical Society Dalton Transactions, 1988, ,	Tj ETQq1 1 1.1	l 0.784314 r 61
550	2453-2465. Synthesis of the dimetal compounds [FeW{μ-PPh2 · CH · CH2 C(C6H4Me-4)}(CO)5(η5-C5Me5)] and [FeMo{μ-PPh2 · CH · CH2 · C(C6H4Me-4)}(CO)5(η5-C5H5)]; molecular structure of the iron-tungsten compound. Polyhedron, 1987, 6, 2067-2071.	2.2	7
551	Chapter 6. Electrochemistry within metal-organic frameworks. SPR Electrochemistry, 0, , 187-210.	0.7	18
552	Electroanalysis with a single microbead of phosphate binding resin (FerrIXâ"¢) mounted in epoxy film. Journal of Solid State Electrochemistry, 0, , 1.	2.5	0
553	Chapter 4. Electrochemistry within nanogaps. SPR Electrochemistry, 0, , 132-154.	0.7	3
554	Solvent-Controlled O2 Diffusion Enables Air-Tolerant Solar Hydrogen Generation. , 0, , .		0
555	CHAPTER 8. Boron in Electroanalysis. Monographs in Supramolecular Chemistry, 0, , 236-255.	0.2	0